RadioGraphics

Imaging of the Female Pelvis through the Life Cycle[1]

Jill E. Langer, MD • Edward R. Oliver, MD, PhD • Anna S. Lev-Toaff, MD Beverly G. Coleman, MD

CME FEATURE

See www.rsna.org/education/search/RG

LEARNING OBJECTIVES FOR TEST 1

After completing this journal-based CME activity, participants will be able to:

- Describe the normal size and appearance of the neonatal and pediatric uterus and ovary.
- Recognize expected physiologic changes in the female pelvic organs throughout the menstrual cycle and after menopause.
- Identify postpartum imaging findings in asymptomatic patients.

TEACHING POINTS

See last page

The appearance of the normal reproductive tract on radiologic images changes dramatically over the female patient's life span, reflecting the influence of hormones on these organs. In female children and adolescents, the appearance of the reproductive tract reflects the stage of sexual maturation. In women of reproductive age, physiologic changes such as those occurring in the corpus luteum are routinely imaged and must be distinguished from pathologic conditions. In the postmenopausal years, as reproductive hormone levels diminish, the endometrium and ovaries undergo progressive involution. Imaging findings that might be considered physiologic in younger women may represent pathologic or even neoplastic changes in postmenopausal women. Although postpartum imaging is typically performed in symptomatic patients, including those with greater than expected vaginal bleeding, suspected obstetric trauma, thromboembolic disease, or infectious complications, clinicians who interpret these radiologic results should be familiar with expected findings in asymptomatic patients after childbirth. Familiarity with the spectrum of ultrasonographic, computed tomographic, and magnetic resonance imaging appearances of the normal female reproductive tract from birth through the postmenopausal years will ultimately help clinicians avoid misinterpreting these normal physiologic changes as pathologic conditions.

Abbreviations: FDG = fluorine 18 fluorodeoxyglucose, IUD = intrauterine device

RadioGraphics 2012; 32:1575–1597 • **Published online** 10.1148/rg.326125513 • **Content Codes:** GU OB

[1]From the Department of Radiology, Perelman School of Medicine at the University of Pennsylvania, 3400 Spruce St, Philadelphia, PA 19104. Received March 12, 2012; revision requested April 13 and received May 8; accepted May 22. For this journal-based CME activity, the authors J.E.L. and B.G.C. have disclosed financial relationships (see p 1595); all other authors, the editor, and reviewers have no relevant relationships to disclose. **Address correspondence to** J.E.L. (e-mail: *Jill.Langer@uphs.upenn.edu*).

Introduction

The imaging appearance of the normal reproductive tract changes over the female patient's life span, largely as a result of the influence of hormones on these organs, especially the uterus and the ovaries. In sexually mature adolescents and women of reproductive age, notable changes in the appearance of the endometrium and ovaries occur on a daily basis. Whether the female pelvis is imaged because of a suspicion of underlying gynecologic disease or as a screening examination in the asymptomatic patient, those who interpret the images should be familiar with the range of normal appearances in these organs to avoid misinterpreting expected physiologic changes as pathologic conditions and to spare the patient unnecessary additional imaging and surgical or other invasive procedures.

Pelvic ultrasonography (US) is the imaging modality most often used for the initial assessment of possible gynecologic abnormalities in patients of all ages. US offers the advantages of widespread availability, low cost, and lack of exposure to ionizing radiation. In appropriate candidates, endovaginal US usually offers higher-resolution imaging than transabdominal US and may be the only examination needed for diagnostic evaluation of the uterus, ovaries, and adnexa. For this reason, the article focuses on the normal appearance of the uterus and ovaries on US images. Magnetic resonance (MR) imaging allows the reconstruction of multiplanar images with a large field of view and excellent soft-tissue contrast and is highly effective in demonstrating normal uterine and ovarian structures. MR imaging is thus an excellent method for imaging evaluation when US is not feasible or the findings at US are inconclusive. Although computed tomography (CT) is not generally considered the primary imaging modality for the evaluation of suspected gynecologic disease, it is commonly performed in patients with acute symptoms. The advent of multidetector CT and the use of multiplanar reformatting offer much-improved depiction of normal female pelvic anatomy when compared with older CT imaging techniques. The article describes the expected findings of normal physiologic changes at US, CT, and MR imaging in healthy female patients of neonatal, pediatric, reproductive, and postmenopausal ages.

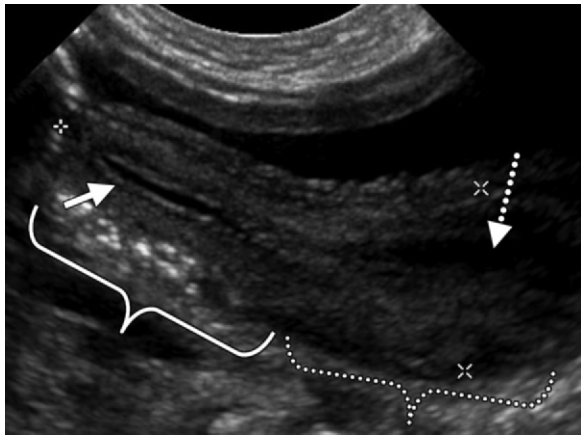

Figure 1. Sagittal transabdominal US image of a normal uterus in a healthy 2-day-old girl. A small amount of fluid noted within both the endometrial canal (solid arrow) and the endocervical canal (dotted arrow) is an effect of maternal hormone stimulation. Note that in the neonatal life stage the normal cervix (dotted bracket) is more prominent and much wider (width marked by calipers) than the uterine body (solid bracket).

Table 1
Normal Uterine Size and Shape by Life Stage

Stage	Uterine Length (cm)	Uterine Body-to-Cervix Ratio*
Neonatal	3.5	2:1
Pediatric	1–3	1:1
Prepubertal	3–4.5	1–1.5:1
Pubertal	5–8	1.5–2:1
Reproductive	8–9	2:1
Postmenopausal	3.5–7.5	1–1.5:1

Sources.—References 1–8.
*Refers to the ratio of the length of the uterine body to the length of the cervix.

Neonatal and Pediatric Life Stages

In infancy, childhood, and adolescence, US is considered the primary imaging technique for evaluation of the reproductive organs and is performed transabdominally, when the urinary bladder is as full as possible. In consenting sexually active youth, endovaginal US is performed. When endovaginal imaging is not feasible, transperineal US can be used.

The neonatal uterus is relatively prominent as a result of exposure to maternal hormones and is well depicted with US. Uterine length in a neonate is approximately 3.5 cm (Table 1),

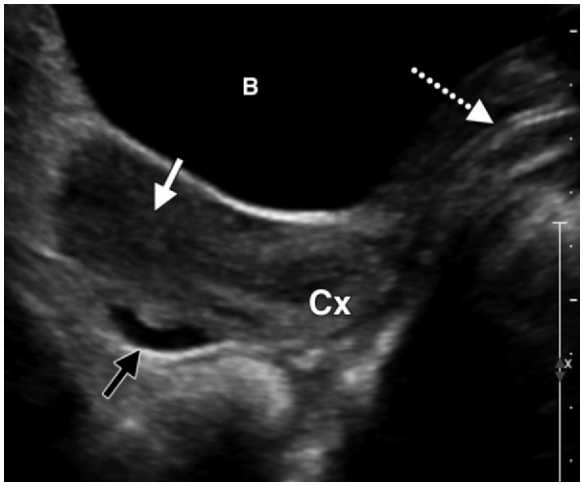

Figure 2. Longitudinal transabdominal US image of a normal uterus in a peripubertal 12-year-old girl. The uterus is less tubular and more pear shaped than in younger children, with the uterine body wider than the cervix *(Cx)*. The endometrium (solid white arrow) is faintly visible and will become more prominent after sexual maturity. The mild angulation of the uterine body with respect to the cervix (ie, anteflexion) seen here is uncommon in younger girls but typical beyond puberty. A small amount of free pelvic fluid (black arrow) can be a normal finding in children of all ages. The vaginal canal (dotted white arrow) is nondistended and appears as two opposed hyperechoic lines representing the mucosal surfaces. *B* = urinary bladder.

and myometrial thickness is about 1.4 cm. The cervix is disproportionately large and bulbous in appearance (1–3). The endometrium appears echogenic, and endometrial fluid is often noted (1) (Fig 1). As hormone levels decrease over the ensuing months, the uterus becomes narrower and shorter, with a mean length of 3.0 cm or less in infants 4–12 months of age, and the cervix becomes equal in proportion to the uterine body, producing a tubular shape (2). The endometrium becomes much less obvious, appearing as a thin echogenic line centrally within the uterus, and is visible with US in only 50% of girls examined at this age (1). The opposed walls of the vaginal canal appear as parallel echogenic linear structures, caudad to the cervix and just posterior to the urinary bladder. In female infants and young girls, reflux of small amounts of urine into the vagina is common, so a minor amount of vaginal fluid is not necessarily indicative of an abnormality (3). A small amount of free fluid in the cul-de-sac is also considered an unremarkable finding in girls of all ages (3) (Fig 2). Beyond 1 year of age, the uterine length gradually increases, with a period of rapid growth as girls approach puberty. The mean uterine length is usually less than 3 cm for young girls, 3–4.5 cm for prepubertal girls, and 5–8 cm for pubertal girls (1,4,5). At puberty, the uterine body becomes thicker and more rounded, described as pear shaped, with a uterine body-to-cervix ratio of approximately 1.5:1, an appearance identical to that in women of reproductive age (2,5) (Fig 2). The postpubertal endometrium is typically easily visible at transabdominal US and varies in thickness with the phase of the menstrual cycle (1,2).

The ovaries likewise vary in size and appearance, depending on the chronologic age of the child and hormonal influences (3–5,9). In neonates, the ovaries typically are located above the level of the true pelvis and are therefore easily imaged transabdominally. As the child grows, the ovaries become situated deeper in the pelvis, most commonly adjacent to the uterus (10).

In premature female neonates, especially those born before 32 weeks of gestation, patency of the processus vaginalis increases the risk for development of an inguinal hernia containing a pelvic peritoneal structure (eg, the bowel, ovary, fallopian tube, uterus). Up to 20% of hernias contain an ovary. Ovary-containing hernias are associated with a greater risk of incarceration than bowel-containing hernias (11).

Gonadotropin levels influence the number of individual follicles and the size of the ovary and stimulate the development of ovarian cysts at all ages (2–5,9,12). The follicle-stimulating hormone level abruptly rises at birth because of the decrease in estrogen and progesterone levels that occurs with separation of the placenta from the neonate, falls to low levels after 3 months of age, and remains low until sexual development begins. Ovarian volume is typically calculated by using the mathematical formula for a prolate ellipsoid, which involves multiplying the product of the three longest diameters (ie, transverse, anteroposterior, and craniocaudal) in centimeters by 0.5233, yielding the volume in cubic centimeters (4). At birth, the typical volume of an ovary is approximately 1 cm^3 but may be as large as 3.5 cm^3 (9,12) (Table 2). The mean ovarian volume remains 1.5 cm^3 or less in girls younger than 7 years and then steadily increases to about 4 cm^3 before puberty, and more than 4 cm^3 after puberty (1,3,4,11,12). The most

Table 2
Normal Ovarian Volume and Appearance by Life Stage

Stage	Ovarian Volume (cm^3)	Ovarian Appearance*
Neonatal	1–3.5	Follicles and cysts common
Pediatric	0.5–1.5	Fewer than six follicles; cysts uncommon
Prepubertal	1–4	Follicles and cysts common
Pubertal	2–6	Follicles and cysts common
Reproductive	4–16	Follicles and cysts common
Postmenopausal	1.2–5.8	Follicles and cysts in approximately 15%–20%

Sources.—References 3,4,7,9,10,12–15.
*Follicles are defined as simple cysts measuring 9 mm or less, and cysts are defined as simple cysts measuring between 9 and 30 mm in menstruating girls and women.

notable increases in ovarian volume occur at two stages: at the onset of thelarche, or breast development, at approximately 8 years of age; and just before the onset of puberty (4).

Both immature and mature ovaries can have follicles in varying stages of development, and these physiologic cysts can be detected at very small sizes with high-resolution US (3,4,9,10,12). Ovarian follicles have been noted at fetal US as early as 28 weeks of gestation (9). Follicles measuring less than 9 mm in greatest diameter are almost always visible in the superficially located neonatal ovary (9,12) (Fig 3). In girls from 1 to 7 years of age, follicles and ovarian cysts are less common; the ovaries may appear homogeneous or have fewer than six visible follicles (3,5) (Fig 4). Ovarian volume greater than 4 cm^3 and the presence of six or more follicles in girls younger than 7 years should raise concern for premature sexual development (5).

Teaching Point

The development of larger physiologic ovarian cysts (greater than 1 cm) can occur in the fetal, neonatal, and prepubertal life stages. Because the risk of malignancy is exceedingly low in children, especially neonates, and most cysts resolve spontaneously, intervention is indicated only when the cyst persists, the patient is symptomatic, or the complexity of the structure raises concern. Small fetal ovarian cysts are considered incidental. However, cysts greater than 4 cm may be associated with an increased risk for in utero torsion; some advocate prenatal aspiration of these large cysts to reduce this risk as well as the risk of compression of adjacent organs or respiratory compromise (9). Approximately 20% of female neonates have ovarian cysts greater than 1 cm, but most ovarian cysts seen in neonates are simple and less than 2.5 cm. Most authors advocate follow-up US for all cysts greater than 2.5 cm and any that contain septa, hemorrhage, or possible solid components. In the neonatal life stage, follow-up and surgical removal of cysts greater than 4 cm to reduce the risk of torsion are controversial. At thelarche and through puberty, follicles and cysts are observed with increasing frequency (4,5).

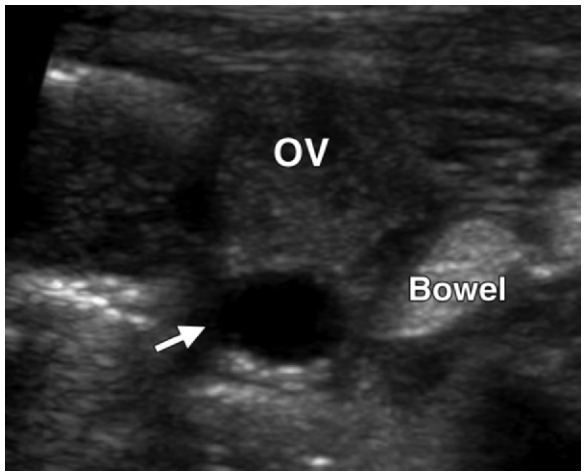

Figure 3. Follicle in the normal ovary of a 2-day-old girl. Transverse transabdominal US image shows an 8-mm, simple-appearing, peripheral follicle (arrow) in the parenchyma of the left ovary *(OV)*. In neonates, the ovaries are usually relatively superficial, lying close to the abdominal wall and above the true pelvis. With high-resolution US, these small follicles are easily seen and can help to identify the ovaries among adjacent bowel loops.

If further evaluation of an abnormality observed at US is needed, MR imaging is the study

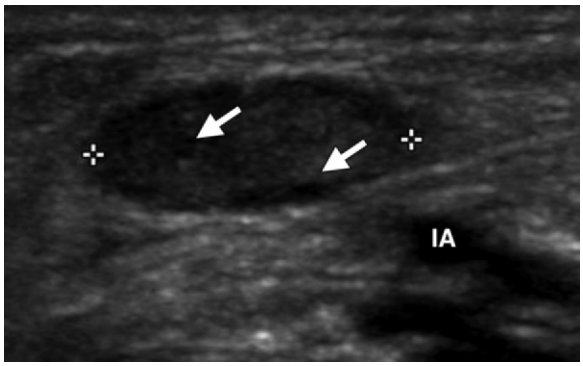

Figure 4. Normal ovary in a 1-year-old girl. Transverse US image of the left ovary (calipers) shows small follicles (arrows), each less than 2 mm. This ovary was easily seen adjacent to the iliac artery *(IA)* by using a high-frequency transducer. In many children, the ovaries are deep within the pelvis and have a homogeneous echotexture that makes visualization of the tiny follicles difficult.

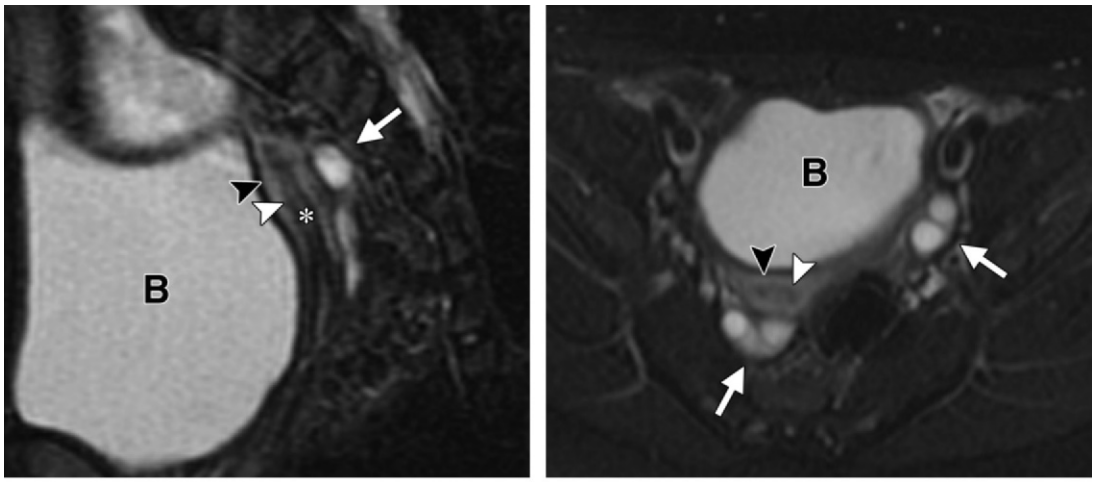

a. b.

Figure 5. Normal uterus and ovaries in a 2-year-old girl. Sagittal **(a)** and axial **(b)** T2-weighted fat-suppressed MR images show the normal configuration of the prepubertal pediatric uterus. In **a**, the uterus is located in its expected position behind the urinary bladder *(B)* and has a tubular configuration, with a uterine corpus-to-cervix ratio of approximately 1:1. The endometrium (* in **a**) is thin and demonstrates high signal intensity. The inner myometrium (white arrowhead) has low signal intensity, and the outer myometrium (black arrowhead) has intermediate to high signal intensity. Although the trilaminar anatomy is well depicted in this case, it can be poorly visualized in prepubertal girls. A few small ovarian follicles are shown (arrows). Fewer than six follicles, appearing as simple fluid-filled cysts less than 9 mm, may be a normal finding in prepubertal girls.

of choice, although infants and young children generally require sedation for the examination. MR imaging is considered preferable to CT because it does not involve the use of ionizing radiation, allows multiplanar image reconstruction, and provides excellent soft-tissue contrast resolution. CT is rarely used to evaluate the reproductive organs in children but may be performed for another indication.

On MR images, the premenarchal uterus tends to have low to medium signal intensity with indistinct zonal anatomy (Fig 5). In pubertal adolescents, the zonal anatomy can be appreciated on T2-weighted MR images. The ovaries appear as ovoid soft-tissue structures most commonly located on either side of the uterus within the mesosalpinx of the broad ligament, paralleling the iliac vessels (16).

On CT scans, the normal uterus has the attenuation of soft tissue and is located just posterior to the urinary bladder. Identification of the uterus and ovaries may be challenging at CT in young, prepubertal girls. As the child ages, the uterus becomes proportionately larger and more easily recognizable. Differential enhancement of the myometrium relative to the endometrium is not usually apparent on CT images until after puberty (16,17). The ovaries are also more easily identified on MR and CT images in adolescents than in girls younger than 8 years, an age when the organs are less likely to contain follicles and cysts (16) (Fig 5).

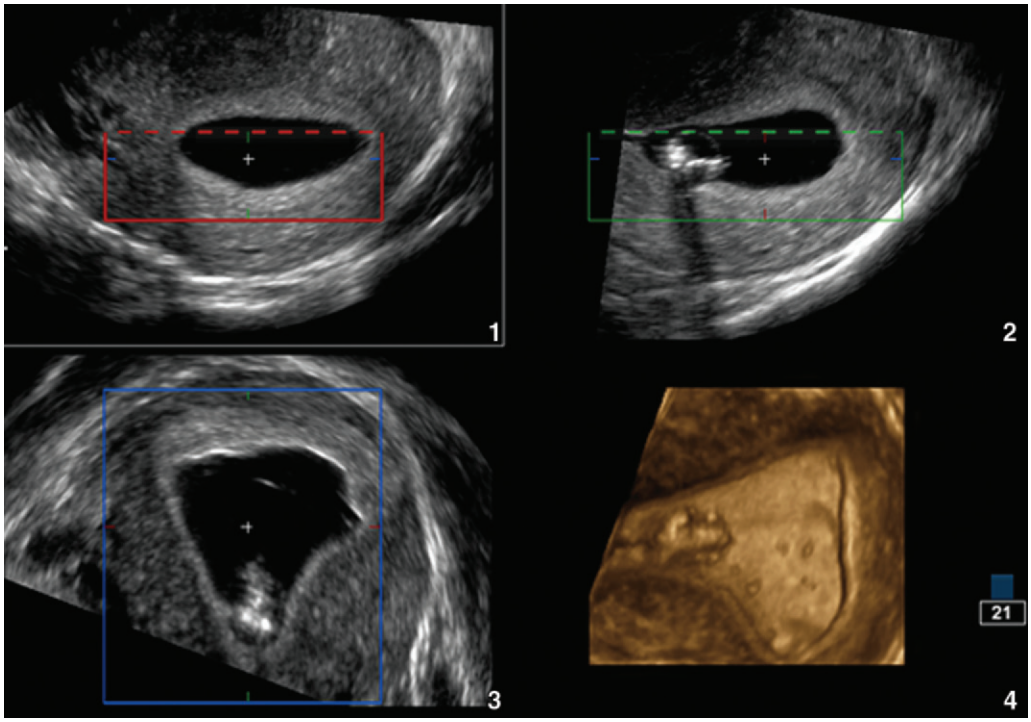

Figure 6. Multiplanar display from hysterosonography performed with a dedicated three-dimensional endovaginal transducer in a 32-year-old woman shows axial (panel 1), sagittal (panel 2), coronal (panel 3), and volume-rendered (panel 4) views. The volume-rendered image was obtained in the midcoronal plane (dashed line in panels 1 and 2). A balloon catheter (seen in the lower uterus in panels 2, 3, and 4) was used to instill saline into and distend the endometrial canal. The normal endometrium appears as a smooth and uniformly echogenic 2-mm band of tissue along the periphery of the triangular cavity in panels 3 and 4. Scrolling through the images obtained at three-dimensional volume-rendered US allows assessment of the entire endometrium. The minimal asymmetry along the left wall has no clinical significance. A few air bubbles, which were inadvertently introduced during the procedure, are most apparent in panel 4.

Reproductive Years

Transabdominal and endovaginal US are the most commonly used techniques for evaluating the pelvis in female patients of reproductive age. Because of its higher resolution, endovaginal US is the preferred technique. When visualization of the uterus at endovaginal US is compromised by large myomas, a high position and fixation due to adhesions, or postpartum enlargement, low-frequency transabdominal imaging may be necessary to examine the entire uterus. In some patients, the use of a combination of techniques is required. The use of three-dimensional volume-rendered US further enhances imaging of the normal female pelvic anatomy by capturing the entire volume of data and permitting display of any desired plane through the uterus, cervix, ovaries, and adnexa (18,19). Because anatomic relationships are more readily comprehended and normal uterine morphology is more easily confirmed at three-dimensional US, the technique is routine in many US laboratories. Assessment of the uterine cavity can be improved with the use of hysterosonography, a technique that involves distending the uterine cavity with the injection of sterile saline or water into the endometrial cavity during an endovaginal US examination (19,20) (Fig 6).

Normal uterine size during the reproductive life stage varies with patient age and parity. The mean dimensions of the normal uterus in women of childbearing age are approximately 8 cm long, 4 cm high, and 5 cm wide, with the multiparous uterus being larger than the nulliparous uterus by as much as 1 cm in each dimension (6). The uterus is typically pear shaped, with the body approximately twice the size of the cervix. The outer contour of the uterine fundus is normally flat or slightly convex superiorly, and the inner myometrial contour facing the endometrial canal is normally flat. The normal shape of the uterine cavity, best displayed in the midcoronal plane at three-dimensional US, is approximately triangu-

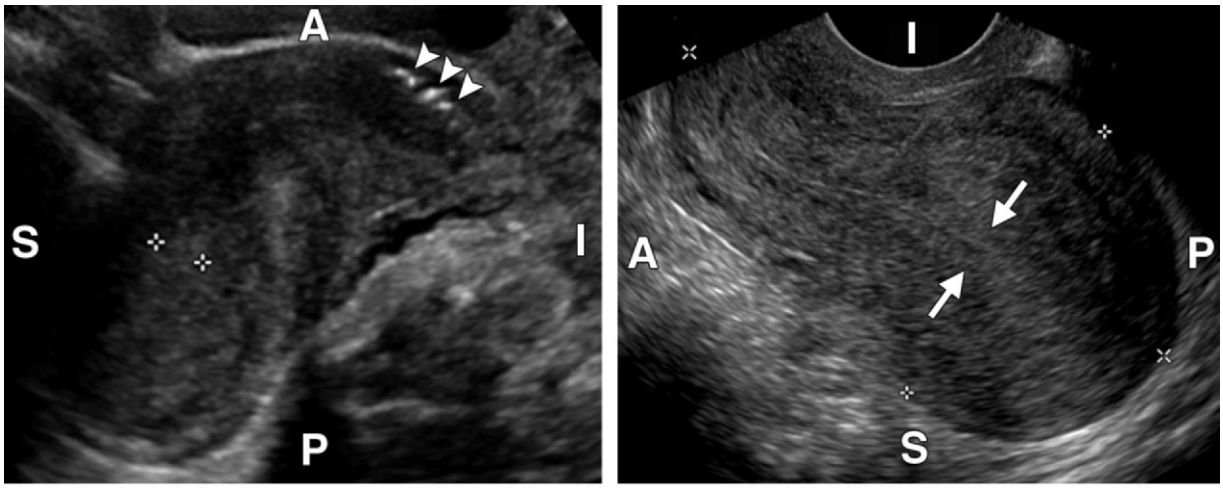

a. b.

Figure 7. Normal uterus in retroflexion in a 28-year-old woman. *A* = anterior, *I* = inferior, *P* = posterior, *S* = superior. **(a)** Midsagittal transabdominal US image shows the uterus in the menstrual phase. The borders of the endometrium were not clearly seen, and the endometrial thickness was thought to measure 8 mm (calipers). The echogenic air bubbles in the anterior vaginal fornix (arrowheads) are related to tampon insertion. **(b)** Midsagittal endovaginal US image obtained in the same woman after voiding shows that the angle of uterine retroversion has increased and the uterine fundus is now oriented toward the patient's feet, at the left of the image. (The endovaginal view is rotated 90° clockwise from the transabdominal view.) The endovaginal view more clearly demonstrates that the endometrial thickness (arrows) is 2 mm, typical of the menstrual phase of the cycle. Note the pear-shaped configuration of the mature uterus, with the uterine body approximately twice the size of the cervix.

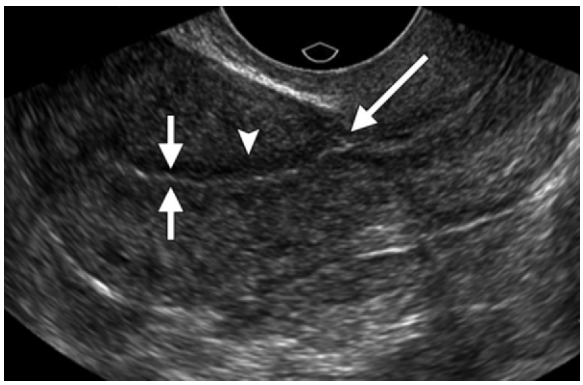

Figure 8. Midsagittal endovaginal US image shows the menstrual-phase endometrium and a scar from a cesarean delivery. The uterus is in anteversion, with the fundus oriented toward the left of the image. The thin and mildly hyperechoic appearance of the endometrium (short arrows) is typical for the menstrual phase. The distinctly hypoechoic subendometrial myometrium (arrowhead) is also visible. Note the tenting of the endometrium anteriorly and thinning of the overlying myometrium at the cesarean scar (long arrow).

lar (Fig 6). The normal uterus assumes a number of positions, which may vary, depending on the degree of distention of the urinary bladder. The positions are described in relation to the angle of the long axis of the uterine body to the long axis of the cervix (flexion) and the long axis of the uterus to the long axis of the vagina (version). The most common position is in anteversion or anteflexion (Fig 2). When the uterus is positioned in retroversion or retroflexion, it may be difficult to image transabdominally and is imaged ideally with an endovaginal transducer (Fig 7). After cesarean delivery, the uterus typically is more elongated, and there is variable deformity or thinning at the site of the lower uterine incision (Fig 8).

During the reproductive life stage, the normal myometrium of the normal uterus has relatively homogeneous echogenicity with smooth outer margins at US. The nongravid uterus is not quiescent but demonstrates myometrial contractions and organized, wavelike endometrial activity with changes in frequency, intensity, and directionality throughout the menstrual cycle. Women with endometrial wave patterns directed from the cervix to the fundus in the periovulatory phase of the menstrual cycle, presumably to promote sperm transport, have been shown to have higher rates of successful fertilization compared with women with uncoordinated or absent wave activity (21). The cervix is homogeneous in echotexture and similar in echogenicity to the uterine body, with a

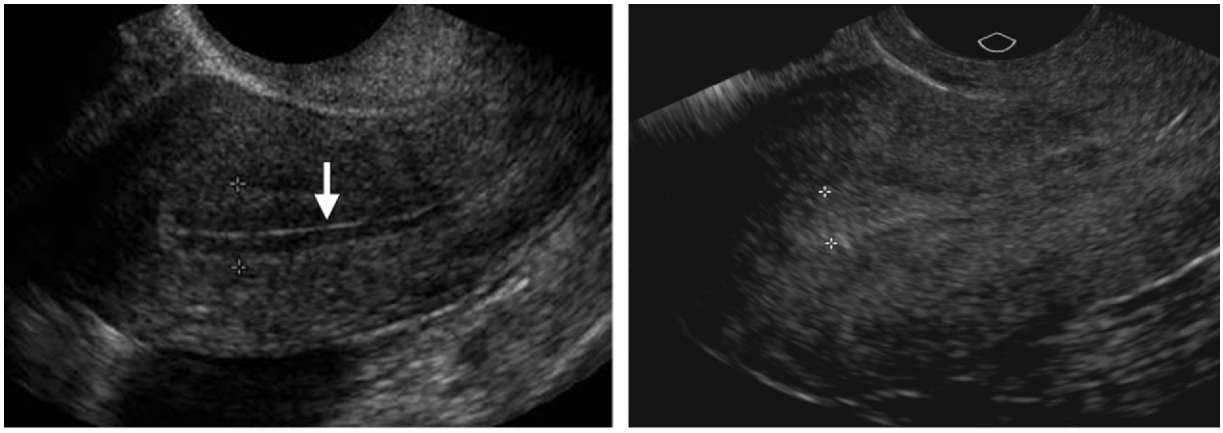

a. b.

Figure 9. Normal endometrium in the middle to late phases of the menstrual cycle. **(a)** Midsagittal endovaginal US image obtained near midcycle shows a normal striated pattern. The endometrial thickness is correctly obtained from the anterior endometrial-myometrial interface to the posterior endometrial-myometrial interface (calipers). At midcycle, this measurement includes the more echogenic outer layer and more hypoechoic inner layer. The thin central hyperechoic line (arrow) is not a layer of endometrium but represents the interface between the anterior and posterior endometrial aspects; it should be continuous when imaged parallel to the long axis of the uterus. **(b)** Sagittal endovaginal US image obtained in a different woman in the secretory phase of the menstrual cycle shows homogeneously echogenic endometrium, which makes visualization of the central interface more difficult. For this reason, assessment of the endometrium for focal abnormalities is best performed in the early phase of the menstrual cycle.

hypoechoic central canal. Nabothian cysts, which are formed by retention of mucus within the endocervical glands, are commonly present in the cervix of parous women. They typically measure less than 2 cm and contain simple fluid, but occasionally contain debris or hemorrhage. The branches of the uterine arteries can be identified on both sides of the cervix at color Doppler flow imaging (22).

Endometrial thickness and appearance vary with the phase of the menstrual cycle. During the menstrual phase (typically days 1–4) and the proliferative phase (typically days 5–13) of the cycle, the endometrium is mildly echogenic and undergoes gradual thickening from a mean of 4.6 mm during menses to 12.4 mm on the day of the luteinizing hormone surge, which occurs 12–48 hours before ovulation (23). During the later portion of the proliferative phase and during the ovulatory phase (days 13–16), the endometrium has a striated pattern, with an inner layer that is relatively hypoechoic surrounded by a more hyperechoic peripheral layer (Fig 9). In the secretory phase of the menstrual cycle (typically days 16–28), the striated pattern is replaced by progressively more homogeneous echogenicity (24), and the endometrial thickness decreases slightly with the luteinizing hormone surge and then increases by about 2 mm (23) (Fig 9). Of note, the day of the luteinizing hormone surge is highly variable, and ovulation may occur as early as day 8 to as late as day 20 in the menstrual cycle of healthy women. For this reason, many authors describe a periovulatory phase that lasts from 6 days before the luteinizing hormone surge until 7 days after it. The appearance and thickness of the endometrium should be considered abnormal if they do not align with expectations for that phase of the menstrual cycle. The appearance and thickness of the endometrium have been correlated with rates of successful implantation and live births, with decreased endometrial thickness and lack of a striated pattern linked to failure to conceive in both spontaneous and therapeutically induced cycles (25).

Teaching Point

Endometrial thickness is best assessed with endovaginal US and represents the sum of the thicknesses of the two endometrial layers. The measurement is obtained on midline longitudinal images by placing cursors at the anterior and posterior endometrial-myometrial interfaces where the endometrium is widest, usually near the fundus. The central thin hyperechoic line represents the interface between the opposing anterior and posterior endometrial layers and should be continuous. Disruption of the central hyperechoic line, or heterogeneity of the endometrium, may indicate an underlying intracavitary lesion such as a polyp, myoma, or adhesion.

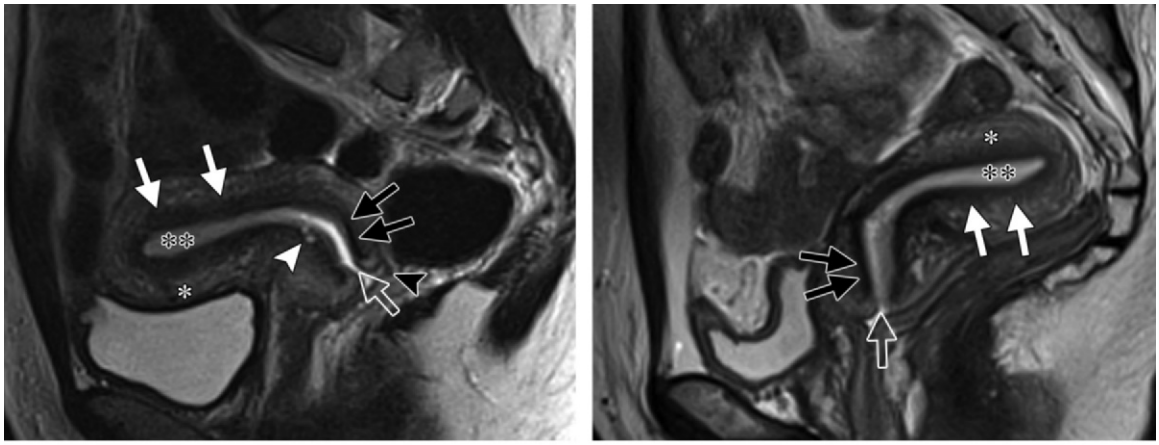

a. b.

Figure 10. Sagittal T2-weighted MR images obtained in two women of reproductive age show normal zonal anatomy of the uterus in anteversion **(a)** and retroversion **(b)**. The endometrium (**) demonstrates signal intensity approaching that of simple fluid and urine in the bladder. The outer myometrium (*) demonstrates intermediate signal intensity, whereas the inner myometrium, or junctional zone (solid white arrows), shows relatively low signal intensity. The normal junctional zone is less than 1.2 cm thick, well marginated, and uniform in thickness. The inner myometrium is contiguous with the fibromuscular stroma in the cervix (black arrows), which has low signal intensity. The external os is also shown (open white arrow). Several small foci of high signal intensity in the lower uterine segment (white arrowhead in **a**) represent small nabothian cysts, a common incidental finding. The posterior vaginal fornix (black arrowhead in **a**) contains a small amount of high-signal-intensity fluid.

The hypoechoic layer peripheral to the endometrium, which is not always visible at US, represents the compact inner layer of myometrium and should not be included in endometrial thickness measurements (26) (Fig 8). A small amount of hypoechoic fluid or mucus within the endometrial cavity or cervical canal is a normal finding, but sizable fluid collections or retained echogenic blood clots may indicate obstructed menstrual flow, as seen with adhesions, cervical stenosis, or excessive bleeding. When fluid is noted in the endometrial cavity, it is excluded from the measurement of the endometrial thickness. In women taking oral contraceptives or using other hormonal contraceptives, such as progesterone-releasing intrauterine devices, the endometrium is generally thin throughout the menstrual cycle.

MR imaging is an excellent tool for evaluation of the uterus. The trilaminar zonal anatomy of the uterine corpus and cervix is well depicted on T2-weighted images (Fig 10). On MR images, the innermost zone of the uterine body represents the endometrium, which demonstrates high T2-weighted signal intensity as a result of mucin-rich endometrial glands. As at US, sagittal views are best for depicting endometrial thickness, which varies with the phase of the menstrual cycle (27). The myometrium has inner and outer layers. The inner myometrial layer, or junctional zone, has low T2-weighted signal intensity because of the presence of compact smooth muscle and low water content, and it is normally less than 1.2 cm thick (28); it is thought to correspond to the hypoechoic subendometrial layer observed at US (29). The outer myometrium demonstrates intermediate T2-weighted signal intensity owing to the presence of less compact smooth muscle, greater water content, and blood vessels (30). The uterine cervix also has a distinct trilaminar appearance on T2-weighted MR images (31). The innermost layer demonstrates high T2-weighted signal intensity that corresponds to the endocervical mucosa and secretions. The adjacent middle layer has low T2-weighted signal intensity that represents predominantly fibrous stroma. The outermost cervical layer demonstrates low to intermediate T2-weighted signal intensity (Fig 10).

On axial CT and MR images, the appearance of the uterus is influenced by the organ's orientation and by the degree of distention of the urinary bladder. The normal-sized uterus positioned in anteversion may be almost entirely imaged within a single axial section (Fig 11). However, if the urinary bladder is greatly distended, the

uterus will align parallel to the long axis of the body, and several sequential images will be required to depict it in its entirety.

Unless recognized as such, the uterus positioned in retroversion can be mistaken for a pelvic mass on CT scans, especially if it displaces or indents the rectum. The normal cervix is often to the right or left of midline and therefore also may be misinterpreted as a mass. Reformatted images in the sagittal plane help demonstrate the position and true length of the uterus and offer the best view for assessing endometrial thickening. On dynamically enhanced, multidetector CT scans, the appearances of the myometrium and endometrium depend on the interval between intravenous contrast material administration and scanning as well as the age of the patient (17,32). On contrast-enhanced CT scans obtained in women of reproductive age, the endometrium exhibits hypoattenuation relative to the inner myometrium during most phases of contrast enhancement, a finding that might be misinterpreted as fluid within the uterine cavity. Such misinterpretation may result in additional, unnecessary imaging examinations or intervention (Fig 12). To date, no criteria have been established for defining normal endometrial thickness on CT images or for distinguishing fluid or blood in the endometrial cavity from endometrial thickening. If there is concern about an endometrial abnormality on the basis of findings at CT, the patient should be referred for endovaginal US. The normal cervix usually demonstrates less intense enhancement or enhances later than the uterine corpus at CT because of the relatively larger proportion of fibrous tissue in the cervix (29) (Fig 13). An intact endocervical canal and a distinct margin between the enhancing myometrium and the hypoenhancing normal cervix at the isthmus help discriminate between the normal cervix and a cervical mass.

Teaching Point

Teaching Point

Normal ovarian volume decreases after the age of 30 years. In a large patient series, mean ovarian volume at endovaginal US was 6.6 cm^3 in women younger than 30 years, 6.1 cm^3 in women 30–39 years old, 4.8 cm^3 in women 40–49 years old, and 2.6 cm^3 in women 50–59 years old. The upper limit of normal ovarian volume in premenopausal women was 20 cm^3 (13). The normal ovary in women of reproductive age also has a variable appearance over the course of the menstrual cycle. Developing and immature follicles can be seen throughout the entire cycle and appear as fluid-filled, unilocular, sharply marginated cysts with diameters of 2–9 mm (Fig 11).

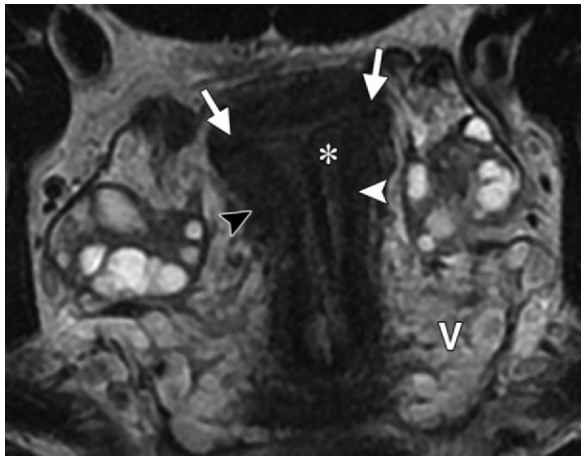

Figure 11. Bilateral ovarian follicles during the early proliferative (follicular) phase in a healthy 19-year-old woman with no history of menstrual irregularity. Axial T2-weighted MR image shows multiple hyperintense ovarian follicles of varying sizes. The zonal anatomy of the ovaries is not well appreciated because of the number of follicles, and although the ovarian volume is greater than the mean for patients of this age, it is within the normal range. Because the uterus is in anteversion, its entire length is visible. The susceptibility artifact (*) is from a plastic progestin-releasing intrauterine device (IUD) centered within the endometrium. Although the IUD is appropriately positioned within the endometrial cavity, the arms extend beyond the endometrium and into the myometrium (arrows), in keeping with minimal myometrial penetration. The uterine shape is normal, with flat external and internal fundal contours. The zonal anatomy is also shown, with a high-signal-intensity endometrium; thin, low-signal-intensity junctional zone (white arrowhead); and intermediate-signal-intensity outer myometrium (black arrowhead). *V* = slow flow within pelvic blood vessels.

In the first half of each menstrual cycle, one or more dominant follicles will grow to a diameter of approximately 20–25 mm and then rupture at ovulation, releasing the oocyte (33). At US, the preovulatory dominant follicle may have a slightly complicated appearance, with the oocyte and its supporting structures (ie, the cumulus oöphorus) appearing as a curvilinear septation within the follicle (Fig 14). After ovulation, the corpus luteum, a remnant of the mature follicle, undergoes a process of cellular hypertrophy and increased vascularization. Therefore, a corpus luteum is typically visible in the secretory phase of the menstrual cycle and persists into the first trimester of pregnancy. On US images, the corpus luteum has a hyperechoic wall that may be slightly irregular in contour, with circumferential low-resistance blood flow at color Doppler flow imaging. Centrally, the corpus luteum may

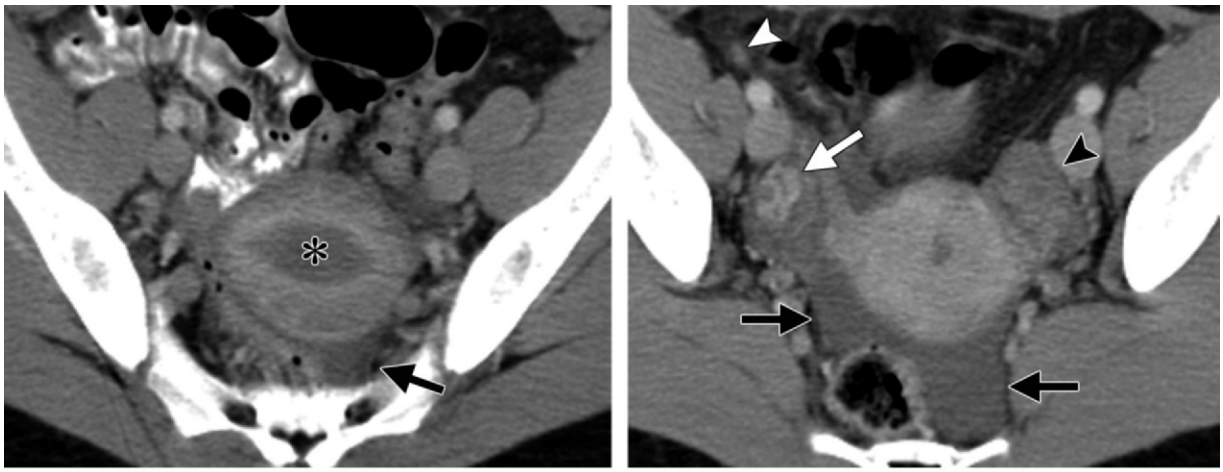

a. b.

Figure 12. Axial contrast-enhanced pelvic CT scans (**a** at a level several centimeters higher than **b**) obtained in a 24-year-old woman with uterine retroversion. **(a)** Image shows hypoattenuation of the endometrium (*) relative to the inner myometrium. The low attenuation of the endometrium, which is in the soft-tissue range, is normal and should not be misinterpreted as fluid in the uterine cavity. The endometrium is relatively thick because it is the secretory phase of the menstrual cycle. Note the displacement of the rectosigmoid junction by the uterus and the small amount of fluid (arrow) posterior to the uterus. **(b)** Image shows the narrower endometrial canal in the lower uterine segment. A moderate amount of fluid in the cul-de-sac (black arrows) is secondary to rupture of the corpus luteum in the right ovary (white arrow). Note the enhanced collapsed wall of the ruptured corpus luteum. The nonovulatory left ovary (black arrowhead) is more homogeneous than the right and has lower attenuation due to fluid-filled follicles. The proximal portion of the right round ligament (white arrowhead) is seen coursing anteriorly.

Figure 13. Midsagittal pelvic CT image shows differential contrast enhancement of the cervix and uterine body in a 23-year-old woman. Because of its fibrous composition, the normal cervix (arrow) is less enhanced than the uterine corpus (arrowhead). The endometrium (*) is normally hypoenhanced relative to the myometrium and should not be mistaken for fluid within the endometrial cavity. Both the length of the uterus and the thickness of the endometrium are well assessed in the sagittal plane.

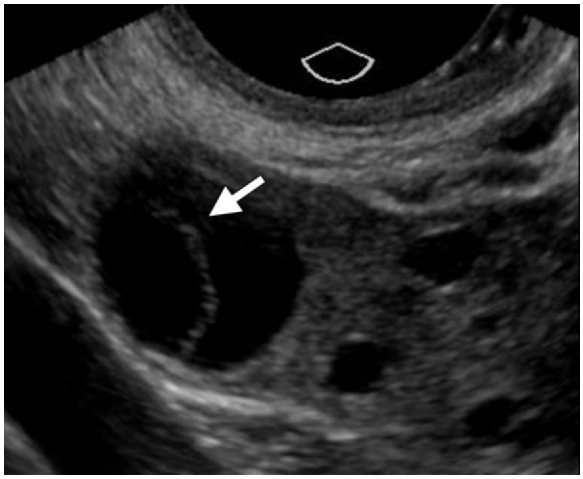

Figure 14. Sagittal endovaginal US image shows a normal dominant follicle and cumulus oöphorus in a 27-year-old woman. The preovulatory dominant follicle is slightly more complicated in appearance than a simple cyst, with the oocyte and its supporting structures appearing as a curvilinear peripheral septum (arrow).

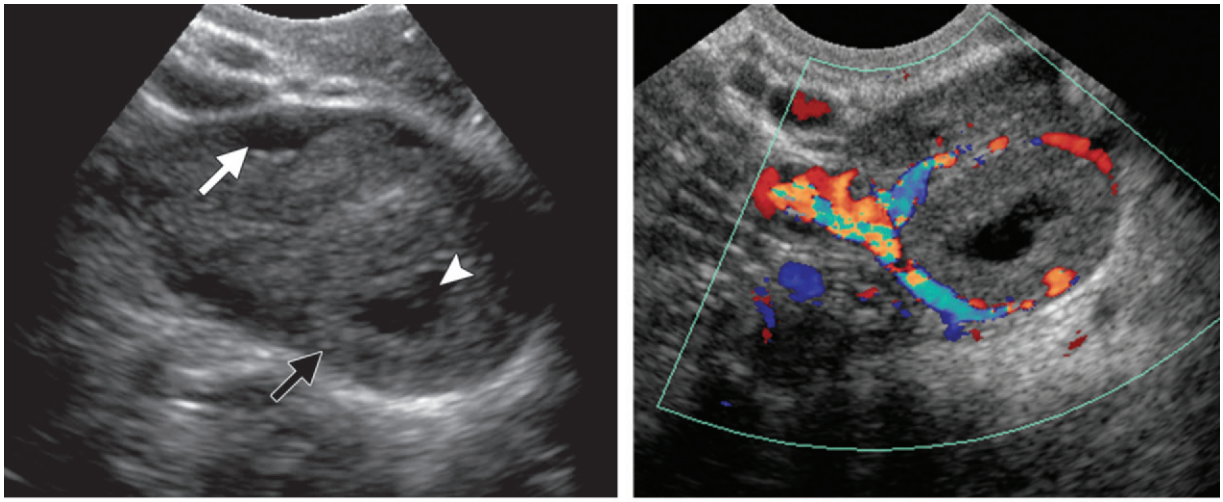

a. b.

Figure 15. Corpus luteum in a 25-year-old woman. **(a)** Transverse US image shows a thick-walled, 2.5-cm corpus luteum (black arrow) within the periphery of the left ovary. A few low-level echoes centrally (arrowhead) likely represent a small amount of hemorrhage that occurred during ovulation. Immature follicles (white arrow), or small simple cysts, appear in the peripheral cortex of the ovary. **(b)** Color Doppler flow image shows marked vascularity only within the wall of the corpus luteum and not in the fluid-containing center.

contain echoes representing internal hemorrhage, but there is usually evidence of increased through-transmission because of the fluid content, and always a lack of central vascularity (Fig 15).

Typically the corpus luteum is less than 3.0 cm in its maximal dimension, reflecting its origin as a follicle, but less commonly it may be larger (34,35). A corpus luteum measuring 3 cm or smaller is considered a normal finding that does not require follow-up imaging (34). In the next cycle, remnants of the corpus luteum may be detectable at US as a small, complex cystic structure, known as an atretic corpus luteum, within the ovary. A corpus luteum that persists beyond the normal duration of 14 days (ie, a persistent corpus luteum cyst) may delay the onset of the next menses by several days or weeks. In a small number of women, a mature follicle sometimes fails to ovulate and continues to enlarge into the next menstrual cycle, occasionally growing larger than 5 cm; these follicles are most often discovered incidentally in asymptomatic women with a clinical history of menstrual irregularity (36). A follicular cyst appears as a simple unilocular or minimally complicated cyst with thin walls, sharply defined borders, and internal fluid. These physiologic lesions should not have internal vascularity. The presence of vascularized solid elements or septa raises the concern that a cyst may be a neoplasm. Although the presence of a large ovarian cystic lesion raises concern for a cystic neoplasm, when no internal vascularity is noted, repeat US performed in the early proliferative phase is recommended after one or two menstrual cycles; many of these structures undergo involution, allowing the diagnosis of a follicular cyst (34). The timing of the follow-up study is intended to help avoid confusion with a newly formed dominant follicle or corpus luteum. A recent consensus statement noted that in women of reproductive age, entirely simple-appearing cysts are almost always benign. Those smaller than 3 cm can be considered a normal finding, those between 3 and 5 cm do not need follow-up, those between 5 and 7 cm should be monitored yearly, and those greater than 7 cm require further evaluation with MR imaging or surgical removal (35).

Teaching Point

At MR imaging, the zonal anatomy of the ovary is best appreciated on T2-weighted images, with the normal medulla showing increased signal intensity relative to the cortex, reflecting the greater amount of loosely packed stroma and blood vessels and diminished cellularity of the medulla (37). After the administration of a gadolinium-based contrast agent, the ovaries typically show less enhancement than the myometrium (38). The presence of ovarian follicles and corpora lutea facilitates identification of the ovaries in women of reproductive age. On T2-weighted images, follicles appear as thin-walled cystic structures with high signal intensity internally; on T1-weighted images, follicles have low to intermediate signal intensity because of internal fluid content (37) (Fig 11). The corpus luteum on T2-weighted images demonstrates a thickened wall with intermediate to low signal intensity that corresponds to a layer of luteinized thecal

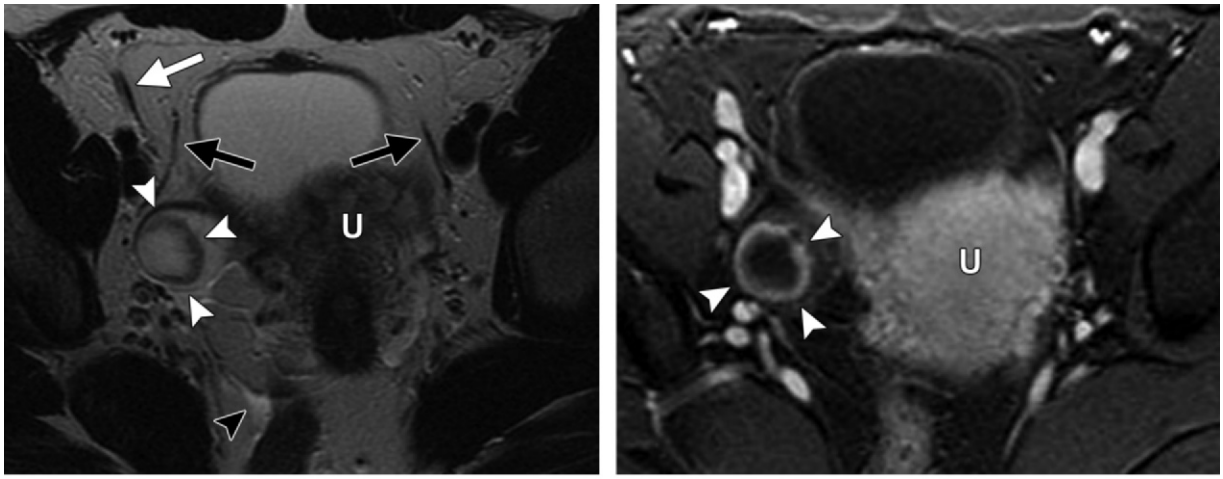

a. b.

Figure 16. Nonhemorrhagic corpus luteum in a 43-year-old woman at midcycle. Axial T2-weighted **(a)** and T1-weighted fat-suppressed contrast-enhanced **(b)** MR images show a right ovarian cystic structure (arrowheads) that represents a nonhemorrhagic corpus luteum. The wall of the corpus luteum, which is composed of a layer of luteinized thecal cells, is thickened and slightly crenated, has intermediate signal intensity in **a** that is higher than that in muscle, and shows avid contrast enhancement similar to that of the uterus *(U)*. The contents of the corpus luteum have T1 and T2 signal intensities similar to those of nonhemorrhagic fluid and urine in the bladder. The right round ligament (white arrow in **a**) courses anteriorly toward the internal inguinal ring, and bilateral medial umbilical ligaments (black arrows in **a**) are seen. A minimal amount of pelvic free fluid with high T2 signal intensity (black arrowhead in **a**) is seen.

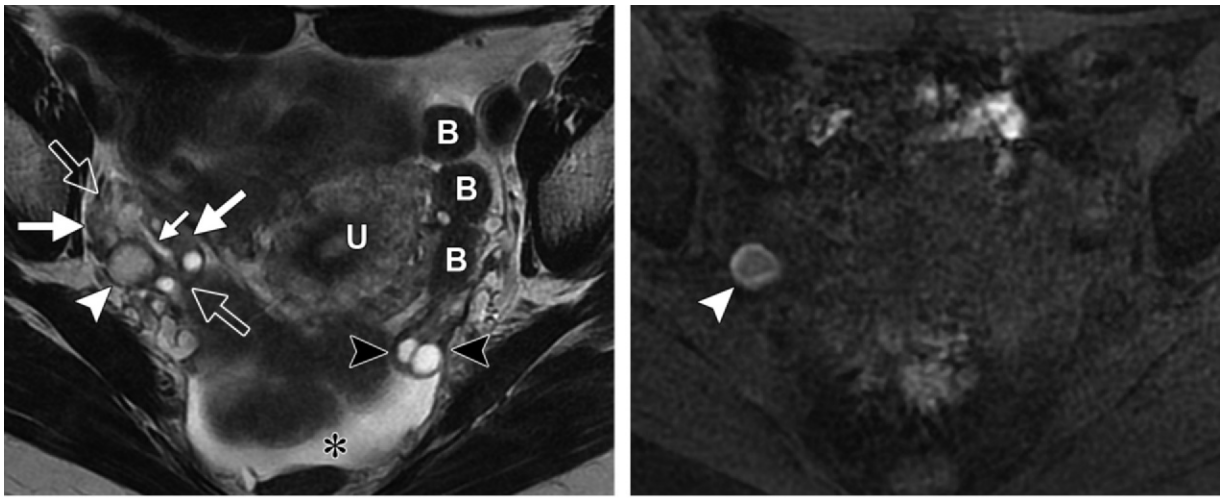

a. b.

Figure 17. Hemorrhagic corpus luteum (hemorrhagic cyst) in a 36-year-old woman. **(a)** Axial T2-weighted MR image shows a right ovarian cystic structure (white arrowhead) with signal intensity higher than normal in a corpus luteum but lower than that of simple fluid in the cul-de-sac (*). The typical zonal anatomy of the right ovary is shown as increased T2 signal intensity within the medulla (small solid arrow) relative to the cortex (large solid arrows), a difference that reflects loosely packed stromal tissue and vessels within the medulla and increased cellularity within the cortex. Note that the physiologically active right ovary (open arrows) is larger than the physiologically inactive left ovary (black arrowheads). *B* = bowel, *U* = uterus. **(b)** Axial T1-weighted fat-suppressed nonenhanced MR image shows high signal intensity of the right ovarian structure (arrowhead), a finding that represents blood products.

cells (37) (Fig 16). In nonhemorrhagic corpora lutea, low T1-weighted signal intensity and high T2-weighted signal intensity are seen. Occasionally, foci of very low T2-weighted signal intensity may be observed along the corpus luteum wall, representing hemosiderin deposition (37). In hemorrhagic or proteinaceous corpora lutea, high T1-weighted and T2-weighted signal intensities are present, and a hematocrit level also may be observed (37) (Fig 17). After the administration

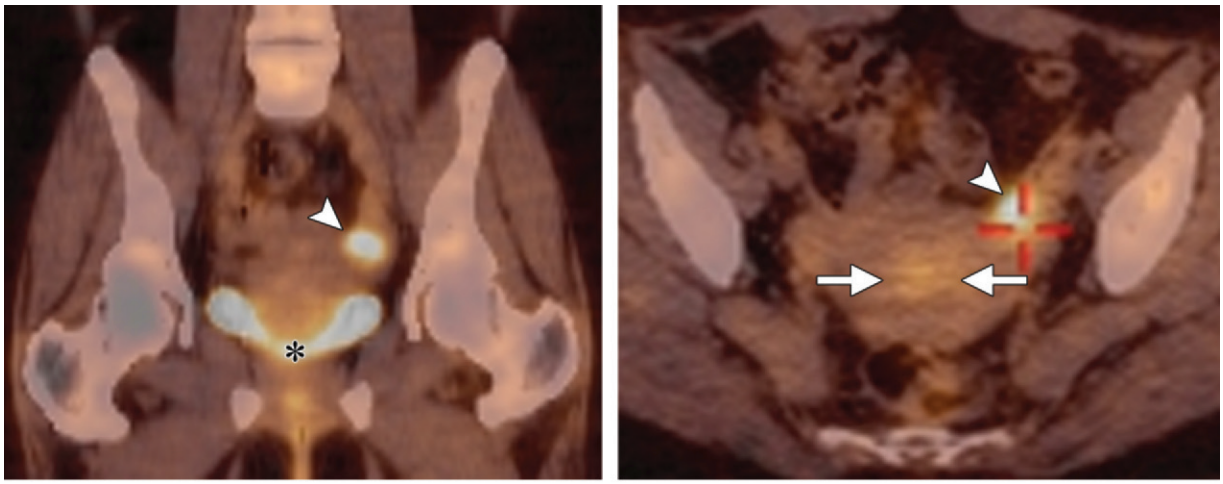

a. b.

Figure 18. Normal physiologic uptake in a 32-year-old woman who underwent FDG PET/CT for poorly differentiated left parotid gland carcinoma. Coronal **(a)** and axial **(b)** fused PET/CT images demonstrate physiologic uptake of FDG representing metabolic activity in the corpus luteum of the left ovary (arrowhead). Trace physiologic FDG uptake in the endometrium (arrows in **b**), a common finding in the late proliferative and early secretory phases of the menstrual cycle, is also shown. Normal excretion of FDG is noted in the urinary bladder (∗ in **a**).

of a gadolinium-based contrast material, avid enhancement of the corpus luteum wall correlates with hypervascularity on color Doppler flow US images. Involuting corpora lutea are decreased in size, and their walls are more convoluted.

On CT images, the appearance of the ovaries depends on the phase of the menstrual cycle, the section thickness, and the timing of the contrast material bolus. In the early reproductive years, the ovaries may demonstrate hypoattenuation relative to the attenuation of other soft-tissue pelvic structures, because of the presence in the ovaries of multiple fluid-filled follicles (Fig 12). With the high resolution afforded by thin-section collimation and dynamic contrast enhancement in multidetector CT, several individual follicles may be apparent within the ovaries. Reformatted coronal CT images can be useful for showing the normal course of the ovarian arteries and veins in relation to the ovary and increasing confidence in its identification. During the ovulatory or postovulatory phase of the menstrual cycle, a corpus luteum with an enhanced rim is evident and sometimes accompanied by adjacent simple or hemorrhagic fluid (39) (Fig 12). Because it is common for women who experience a symptomatic cyst rupture to undergo CT, those interpreting the images should be alert for an intact or rupturing corpus luteum and thus avoid misinterpretation or inappropriate management of these findings.

The normal fallopian tube is difficult to distinguish from surrounding vessels and ligaments at imaging. The tube is not usually visualized on US images unless it is abnormal or surrounded by fluid. Occasionally, it can be seen as an elongated structure adjacent to the ovary. The normal fimbriae can be seen as short echogenic fingerlike projections when surrounded by periovulatory fluid or at hysterosonography. The round ligament is often observed on CT and MR images; it is distinguished from the fallopian tube by virtue of its anterior course to the internal inguinal ring (Fig 12).

At positron emission tomography (PET), uptake of fluorine 18 fluorodeoxyglucose (FDG) as a result of normal physiologic function in the ovaries and especially in the corpus luteum is common in women of reproductive age who undergo imaging in the late follicular and early luteal phases of their cycle. The uptake typically appears as a unilateral round or ovoid region of intense focal activity with a standardized uptake value greater than 3.0 (Fig 18). Cyclical endometrial uptake has also been noted at PET, most often during the ovulatory phase and during menstruation. Dual-modality imaging with CT (ie, PET/CT) helps show the characteristic features of these physiologic changes and the absence of features suggestive of malignancy. To minimize the potential for misinterpretation of results in women of reproductive age, PET examinations should be conducted within a week before or a few days after menses (40).

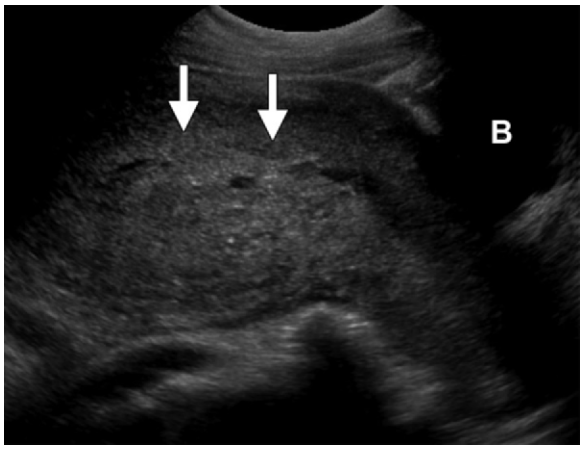

Figure 19. Normal postpartum uterus in a 26-year-old woman. Midline sagittal transabdominal US image obtained 3 days after vaginal delivery shows an enlarged uterus with echogenic material (arrows) presumably representing blood products within the endometrial canal. The myometrium has a heterogeneous echotexture, and the inner and middle portions of the endometrium are hyperechoic in comparison with the outer myometrium. This common early postpartum appearance makes it difficult to distinguish endometrium from myometrium. *B* = urinary bladder.

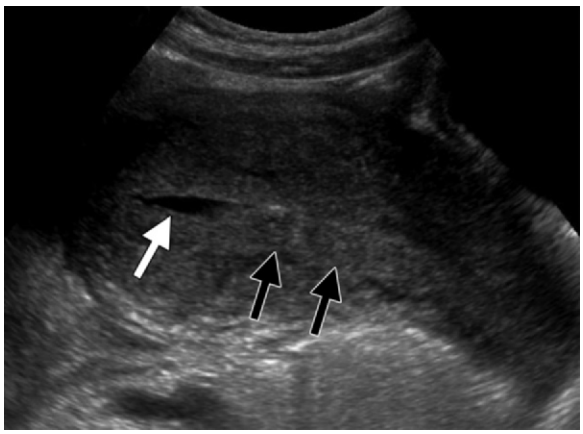

Figure 20. Postpartum uterus in a 28-year-old patient with greater than expected vaginal bleeding. Midline sagittal transabdominal US image of the uterus obtained 15 days after vaginal delivery shows both simple fluid (white arrow) and echogenic material (black arrows) within the endometrial canal. Treatment was conservative, and the patient's symptoms subsided. Fluid and echogenic material are noted in 75% of asymptomatic women 14 days after vaginal delivery, and these findings are not necessarily indicative of underlying disease.

Postpartum Life Stage

Puerperium is the period 6–8 weeks after delivery when the uterus undergoes physiologic involution and returns to the nongravid state. The most rapid changes occur in the first few days after delivery. The uterus is approximately 20 cm in length and weighs about 1 kg immediately after childbirth but decreases by approximately 50% in the next 24–48 hours (41–45). Beyond the first few days postpartum, the uterine involution is more gradual, with the uterus measuring 11.2 cm long at 3 weeks and 8.7 cm long at 6 weeks postpartum. The timing of the involution may be prolonged in multiparous women and shorter after preterm delivery, but it is not usually affected by infant birth weight or breast-feeding (41). Within the first few days after delivery, the remaining superficial decidual tissue becomes necrotic and is sloughed in the lochia. The deeper decidual layer proliferates and restores the endometrium by 3–6 weeks postpartum (42).

On US images, the immediate postpartum myometrium often appears heterogeneous and has higher echogenicity than the myometrium of a nongravid uterus (41,42) (Fig 19). Increased diffuse and focal myometrial vascularity at the placenta insertion site has been described in the absence of abnormal postpartum bleeding (42,43). Intracavitary fluid, blood products, and small amounts of gas are commonly noted in asymptomatic women after delivery and therefore are not necessarily indicative of a postpartum complication. Fluid and echogenic material are noted in the endometrial cavity of 20% of asymptomatic women in the first few days after vaginal delivery, and these findings are even more common at 1 week postpartum, being present in approximately half of women examined (41,43,44). The amount of blood products diminishes over the ensuing weeks, but complex fluid may still be present in 6% of women 3 weeks after vaginal delivery (42–44) (Fig 20). Hyperechoic foci on US images, likely representing intracavitary gas, have been noted in asymptomatic women as late as 3 weeks after vaginal delivery and are noted after both vaginal and cesarean deliveries (41–44,46) (Fig 21). Because US is not commonly used to

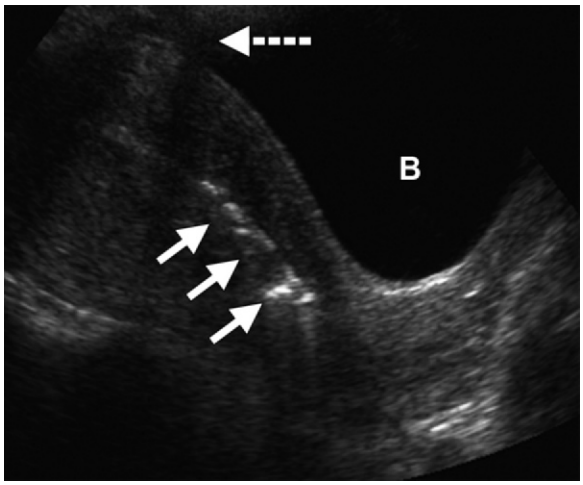

Figure 21. Postpartum uterus in a 34-year-old woman. Midline sagittal transabdominal US image obtained 5 days after vaginal delivery shows an enlarged uterus with markedly echogenic material (solid arrows) within the endometrial canal of the lower uterine segment, presumably representing gas; the patient had no clinical symptoms suggestive of endometritis. Intraendometrial gas may or may not produce distal acoustic shadowing at US and has been reported in asymptomatic women as long as 3 weeks after delivery. An echogenic focus producing distal shadowing (dashed arrow) within the urinary bladder *(B)* is also likely gas, as the patient underwent bladder catheterization before this examination.

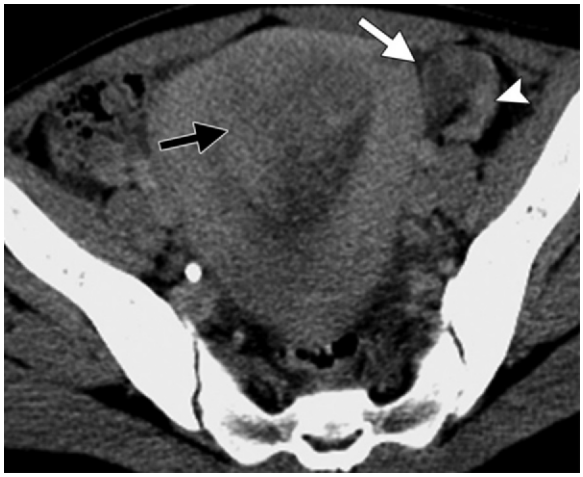

Figure 22. Normal enlarged postpartum uterus in a 27-year-old woman. Axial contrast-enhanced CT image obtained 4 days after vaginal delivery shows an expanded uterus containing heterogeneous material (black arrow) of mixed attenuation, presumably blood products, within the canal. A normal left ovary (white arrow) and enhanced gonadal vein (arrowhead) are also shown.

evaluate asymptomatic patients after cesarean delivery, relatively few articles describe the expected extrauterine findings. At US performed in women 4 days after surgical delivery, abdominal wall collections were observed in 40% and pelvic collections in fewer than 10%. Notably, neither the presence nor the absence of these collections was predictive of febrile morbidity (47).

At CT performed in the first few days after a vaginal delivery, the uterus is enlarged and may show marked myometrial enhancement. In asymptomatic women, the endometrial canal may contain fluid, lochia, and small amounts of gas and is usually less than 2 cm in maximal width. Larger amounts of gas, fluid, or soft tissue require clinical correlation to exclude endometritis and retained products of conception (48) (Fig 22). MR imaging typically demonstrates heterogeneous myometrial signal intensity, prominent vascularity, and endometrial blood products (49–51). High signal intensity in the outer cervical stroma on T2-weighted images may also be noted, likely reflecting edema from mechanical stress of the fetal head on the cervix (49). Parametrial edema unrelated to deep pelvic infection or ovarian vein thrombosis has also been noted on MR images (49) (Fig 23). Free pelvic fluid and small hematomas are not usually seen on CT scans performed after uncomplicated vaginal delivery but have been reported more commonly on MR images, likely reflecting the latter modality's high sensitivity for small amounts of fluid (49,50). After cesarean delivery, both CT and MR images can be expected to show free pelvic fluid and small loculated pelvic fluid collections in most asymptomatic patients (48,49,52).

Postmenopausal Life Stage

Menopause refers to the permanent cessation of menstruation in female humans with an intact uterus. In Western countries, the average age at onset of menopause is between 51 and 53 years, with a range of 40–60 years (53,54); onset is affected by many factors, including smoking, race, ethnicity, and body mass index (55,56). A strict determination of menopausal status is difficult, as the process represents a continuum that begins with perimenopause, a time span in

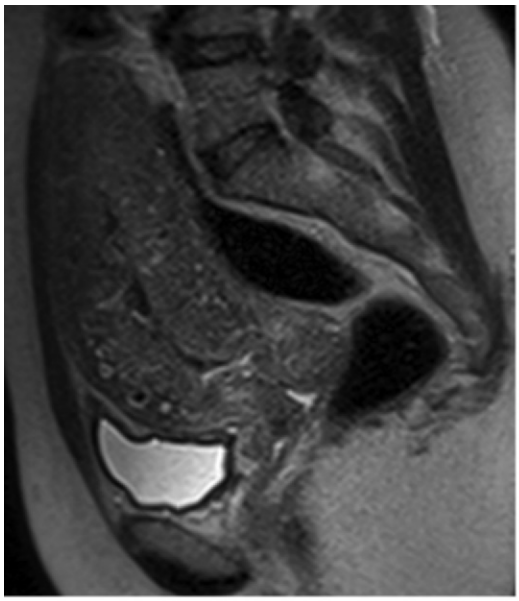

a.

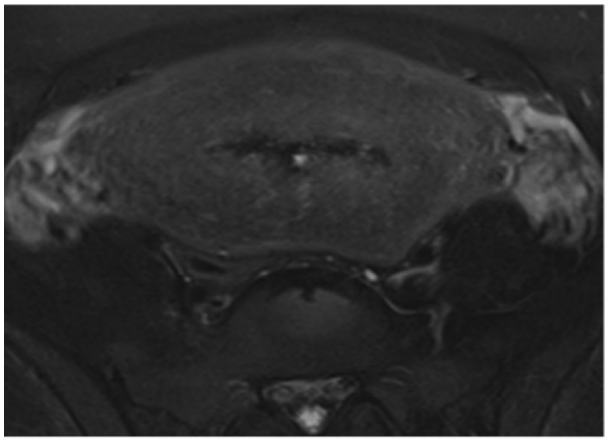

b.

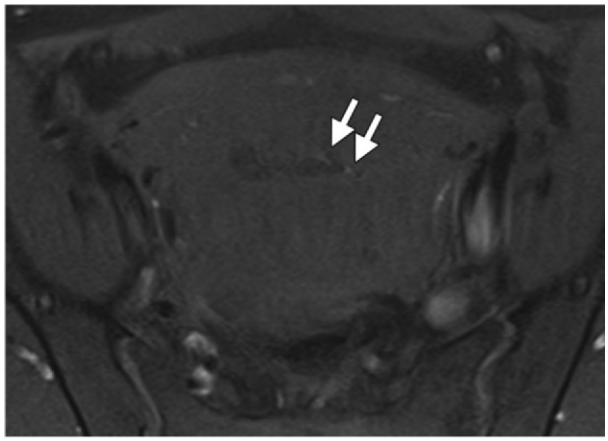

c.

Figure 23. Edema in the uterus of a 33-year-old woman who underwent pelvic MR imaging for another indication 1 day after a normal vaginal delivery. Sagittal T2-weighted **(a)**, axial T2-weighted fat-suppressed **(b)**, and axial nonenhanced T1-weighted fat-suppressed **(c)** images show an enlarged postpartum uterus. The T2-weighted images **(a, b)** demonstrate diffuse myometrial and cervical edema, which appears as high signal intensity. Bilateral parametrial regions with high signal intensity representing edema are seen in **b**. A few small foci of blood products within the endometrial cavity (arrows in **c**) are expected findings.

which the patient experiences menstrual cycles of variable length and volume of flow, often with skipped cycles. Patients are officially deemed postmenopausal when they have experienced amenorrhea for 12 consecutive months from the date of the last menstrual flow, although sporadic ovulatory cycles have been reported rarely in postmenopausal women (57).

Pelvic US is well recognized as the primary imaging modality for initial evaluation of postmenopausal status. Although transabdominal US performed with the full bladder technique allows diagnostic imaging in some postmenopausal women, the modality has limitations. Transabdominal pelvic US may be compromised by a variety of senescent changes, including decreased urinary bladder capacity, increased body habitus, an atrophic and ill-defined endometrial canal, small ovarian volume, and absence of ovarian follicles. In many postmenopausal women, endovaginal US is required to adequately image the endometrium and ovaries. Fortunately, postmenopausal patients tolerate the endovaginal examination, with an overall patient acceptance rate that is only slightly lower than that among women of reproductive age. Transrectal US also may be performed to view the uterus and adnexal structures.

Because of the smaller size of the postmenopausal uterus, it can often be shown at imaging in its entirety, from the cervix to the fundus, regardless of the degree of uterine version or flexion (Fig 24). The most rapid decline in uterine size occurs within the first 10 years after menopause,

with a more gradual decline thereafter (7,8). The uterus ranges from 3.5 to 7.5 cm in length and from 1.2 to 3.3 cm in anteroposterior diameter in patients older than 65 years (7), with the wide ranges reflecting variations in patient parity, the number of years since the onset of menopause, and the presence of preexistent uterine disease such as adenomyosis and myomas.

The myometrial appearance is often more heterogeneous in postmenopausal women than in premenopausal women, and the uterine body-to-cervix ratio in postmenopause approaches 1:1. Calcified uterine arcuate vessels are commonly noted in elderly postmenopausal women, especially those with diabetes, vascular disease, hypertension, or hypercalcemia (58). These vessels appear in the superficial myometrium as peripheral linear reflections with a circumferential pattern that helps distinguish them from calcified myomas, which tend to have curvilinear calcifications with dense shadowing (Fig 25). Nabothian cysts are frequently present in the cervical region of postmenopausal patients and are usually smaller than those observed in younger women. Free peritoneal fluid is occasionally seen in postmenopausal women and is not necessarily pathologic when small in amount and simple in appearance, especially in early menopause. Free fluid in late menopause is abnormal and could be related to a variety of conditions, including intraperitoneal malignancy and ascites due to cardiac, renal, and liver disease.

The postmenopausal endometrium is typically atrophic because of the lack of estrogen stimulation and appears as a thin hyperechoic line or band measuring only 1–2 mm in maximum diameter (6) (Fig 24). As in women of reproductive age, the endometrial thickness (the sum of the two endometrial layers) should be obtained with digital calipers on a longitudinal endovaginal US image at the site of maximum thickness, which is usually at or just below the uterine fundus (59,60). The relatively vascular and compact inner myometrial layer, which surrounds the endometrium and appears hypoechoic, should not be included in the measurement. A small amount of endometrial fluid, less than 2 mm in diameter, may be seen in a postmenopausal patient with an otherwise normal uterus, usually as a result of mild cervical stenosis. This fluid should be excluded from the endometrial thickness measurement (Fig 26).

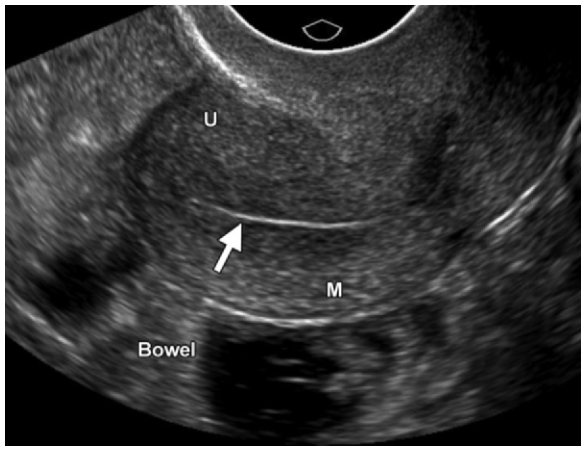

Figure 24. Normal endometrium in a 58-year-old woman with vaginal bleeding 6 years after the onset of menopause. Sagittal endovaginal US image shows anteversion of the uterus *(U)* with an atrophic, thin endometrium (arrow) measuring 1 mm in thickness. The myometrium *(M)* has a slightly coarse, speckled echotexture, a common appearance seen in postmenopausal women. Endometrial disease can be excluded with a high degree of certainty; the most likely cause of the bleeding is endometrial atrophy.

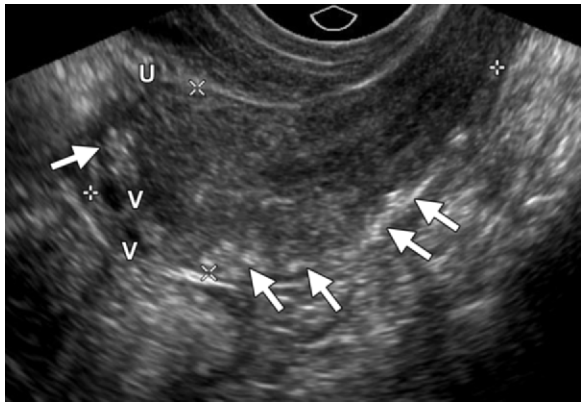

Figure 25. Arcuate vascular calcifications in an 81-year-old woman with postmenopausal bleeding. Sagittal endovaginal US image shows anteversion of the uterus *(U)* with extensive arcuate artery calcifications (arrows). The endometrium, which is only faintly visible on this image, was 2 mm thick, a decrease from previous measurements; this finding was consistent with endometrial atrophy. *v* = adjacent arcuate veins.

US plays an important role in the evaluation of possible endometrial disease in both symptomatic and asymptomatic postmenopausal patients (61–63). A normal endovaginal sonogram in a postmenopausal patient has a high negative predictive value and high overall accuracy rate for excluding major disorders of the uterus and ovaries, with excellent pathologic correlation

Teaching Point

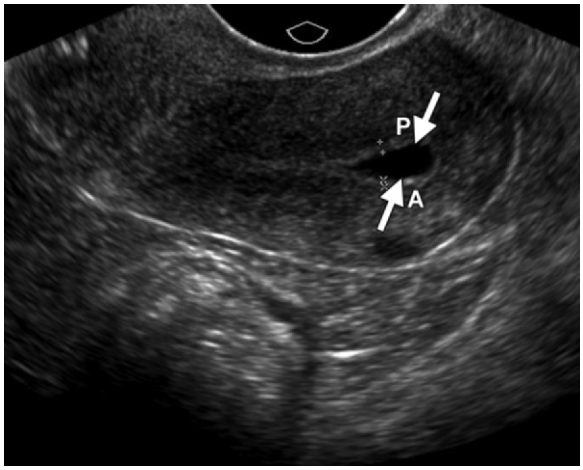

Figure 26. Simple endometrial fluid in a 66-year-old asymptomatic woman with a 3-year history of breast cancer treated with lumpectomy and radiation. Sagittal endovaginal US image shows retroversion and retroflexion of the uterus with a small amount of simple endometrial fluid (arrows) near the fundus. An endometrial thickness of 1.7 mm was determined by adding 0.7 mm for the anterior *(A)* layer to 1.0 mm for the posterior *(P)* layer.

(61,62). It has been shown that measurements of the endometrium obtained with endovaginal US are within 1 mm of those obtained at pathologic examination (61) and that regardless of symptoms, an endometrial thickness of 5 mm or less is associated with benign histopathologic findings in most cases. This threshold serves as a useful guide for determining which patients should undergo endometrial biopsy. The risk of missing an endometrial abnormality with use of a single measurement of 5 mm or less at endovaginal US is low, with a 99% negative predictive value for endometrial cancer (61–63). Therefore, postmenopausal patients who present with vaginal bleeding and have an endometrial thickness of 4–5 mm or greater should be referred for further evaluation to exclude endometrial carcinoma. In postmenopausal patients without abnormal bleeding, most experts advocate tissue sampling only when the endometrial thickness exceeds 8 mm, as the risk of clinically significant endometrial abnormalities in these patients is low. In postmenopausal patients without vaginal bleeding and with an endometrial thickness from 5 to 8 mm, treatment should be based on individual symptoms and risk factors. Because endovaginal US can be used to accurately assess the endometrium, sequential US examinations can be of value for close monitoring of endometrial thickness (62).

Hormone replacement therapy affects the thickness of the endometrium. Sequential estrogen and progesterone therapy, often used in perimenopausal patients in the United States, induces cyclical endometrial changes and symptoms similar to those occurring in premenopausal patients. In such cases, US scans should be obtained early in the cycle or near the end of withdrawal bleeding, when transient physiologic thickening is not expected to be present. The use of continuous estrogen and progesterone regimens leads to endometrial atrophy; therefore, measurements of endometrial thickness in these patients are usually within the normal range (61). Unopposed estrogen therapy is associated with an increased risk of endometrial hyperplasia or carcinoma and is typically prescribed only for posthysterectomy patients (64). Tamoxifen has been proven effective for the treatment of breast cancer but is associated with increased incidence of endometrial disease among postmenopausal women because of its estrogenic effect on the uterus. Several studies have shown a direct correlation between the use of tamoxifen and an increase in endometrial thickness, most notable beyond 3 years of therapy (59,60,65). Nearly half of all postmenopausal women undergoing tamoxifen therapy have an endometrial thickness greater than 8 mm, and most are asymptomatic, without abnormal vaginal bleeding (59,60,65). The most common histopathologic findings, including hyperplasia and polyps, are benign, with an approximate 1% risk of endometrial carcinoma (59,60,65). Because endometrial thickening is commonly due to benign causes in patients receiving tamoxifen therapy, there is no consensus about a threshold thickness for recommending endometrial sampling in asymptomatic women (61).

The postmenopausal uterus is similarly atrophic on CT and MR images. The endometrium may occasionally be identified on contrast-enhanced CT images and should appear thin, regular, and hypoenhancing relative to the myometrium (32,61). Patients with an abnormal endometrial appearance at CT should be referred for further evaluation with endovaginal US. The uterine zonal anatomy in postmenopausal women is usually indistinct or absent, but if present, it is best evaluated on T2-weighted images, as in women of reproductive age (Fig 27). The normal postmenopausal endometrium has hyperintense signal on T2-weighted MR images and should be no more than 5 mm thick (66).

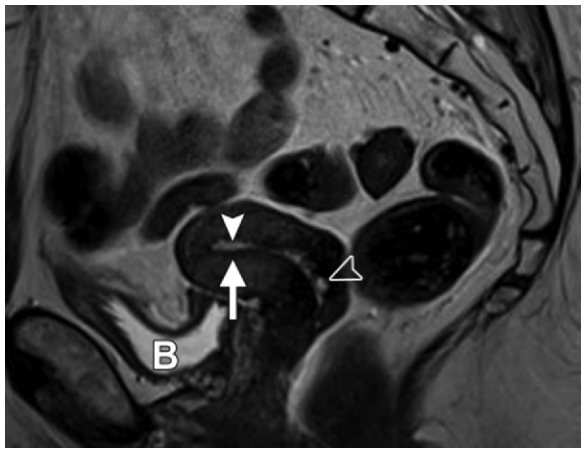

Figure 27. Sagittal T2-weighted MR image obtained in a 60-year-old woman 3 years after menopause reveals a small uterus with a normal, thin (<4-mm), hyperintense endometrium (solid arrowhead) and barely perceptible hypointense junctional zone (arrow). A small nabothian cyst (open arrowhead) is also shown. Note that the uterine corpus has undergone some atrophy and is only slightly bulkier than the cervix. In late menopause, the uterine corpus is smaller than the cervix, and the uterine zonal anatomy may be difficult to appreciate. *B* = bladder.

The normal postmenopausal ovary is less echogenic, is smaller, and generally has fewer follicles than the normal ovary during the reproductive years. As a result, the ovaries may be difficult to detect at both transabdominal and endovaginal US (67). Small (1–3-mm) punctate echogenic foci with no associated soft-tissue mass may be seen in postmenopausal ovaries, most often in the periphery. These foci may be dystrophic calcifications in atretic follicles and surface epithelial inclusion cysts or may be tiny cystic spaces producing reverberation artifact (68,69). In postmenopausal women, as in patients of reproductive age, such findings often are of no clinical significance and can be reevaluated with follow-up US if there is concern or uncertainty about their origin. The uterus is an important landmark, and the broad ligaments can often be traced to the ovaries, which are attached to the posterior aspect of the ligaments. Pelvic vessels or stationary bowel loops may be mistaken for postmenopausal ovaries, and the sonographer may need to use color Doppler flow imaging or exert manual pressure on the abdominal wall to displace the bowel loops and improve visualization of these small structures.

Ovarian size correlates with hormonal status and duration of menopause. Mean postmenopausal ovarian volumes have ranged from 1.2 to 5.8 cm^3, with an ovarian volume greater than 8 cm^3 considered abnormal in all cases (14,15). Some authors have suggested that an ovary that is twice as large as the contralateral ovary, regardless of absolute size, should be considered abnormal (14).

Even though folliculogenesis has ceased, the postmenopausal ovaries are not as quiescent as initially thought. Simple ovarian cysts as large as 3 cm have been reported in as many as 15% of postmenopausal patients; most such cysts spontaneously regress, as verified at serial US examinations (35,70,71). The simple cyst seen at imaging in early menopause probably represents an occasional ovulatory event or an atretic follicle. However, any anechoic lesions in postmenopausal ovaries should generally be referred to as *cysts* (35). Although ovulation is rare in late menopause, smaller cysts less than or equal to 1 cm in diameter have been seen in as many as 21% of patients (70,71). These cysts are more readily observed with endovaginal US than with transabdominal US because of the high resolution provided by the endovaginal transducer in proximity to the small postmenopausal ovaries (Fig 28). Simple-appearing cysts smaller than 1 cm do not need further follow-up, and their description should be included in the final report at the discretion of the interpreting physician (35).

The postmenopausal ovaries may be similarly difficult to identify at MR imaging and CT because of atrophy and the paucity or absence of follicles and cysts that help localize the structures in patients of reproductive age. At MR imaging, the ovaries demonstrate homogeneous intermediate to low signal intensity on T1-weighted images and decreased signal intensity on T2-weighted images, possibly because of a reduction in the number of fluid-containing follicles in the medulla and an increased number of stromal cells (38) (Fig 29). After contrast material administration, the ovaries demonstrate enhancement similar to or less than that seen in the uterine myometrium (38). Small epithelial inclusion cysts may occasionally be seen in the postmenopausal ovary and typically appear as subcentimeter, unilocular, hyperintense cystic structures on T2-weighted images (38). On CT scans, the postmenopausal ovaries typically appear as small and relatively featureless triangles or flattened soft-tissue structures, often adjacent to the uterus or iliac vessels. Identification of the ovaries on coronal reformatted images may be facilitated by following the gonadal vessels into the pelvis.

Conclusion

The uterus and ovaries undergo remarkable changes in size and appearance over the course of a lifetime. A thorough knowledge of how hormonal changes affect the appearance of the uterus and ovaries at pelvic imaging performed in childhood,

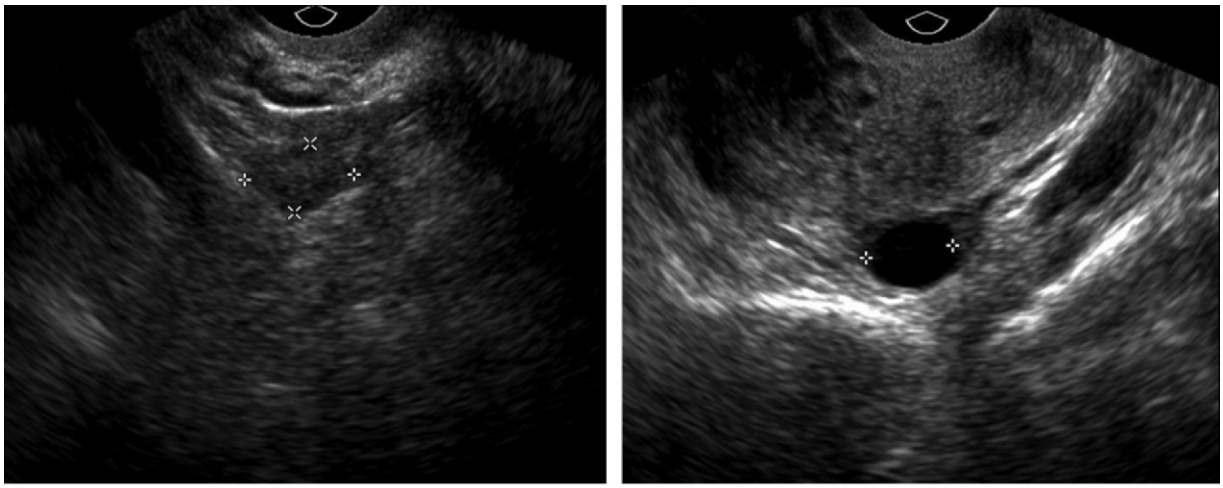

a. b.

Figure 28. Simple ovarian cyst in a 61-year-old woman 10 years after menopause. **(a)** Sagittal endovaginal US image shows an atrophic right ovary (cursors) with a calculated volume of 4 cm^3. A few tiny follicles are barely perceptible. **(b)** Coronal endovaginal US image of the left ovary shows a simple-appearing 1.3-cm cyst (cursors) that had remained unchanged for 2 years. The ovary was located deep in the pelvis, posterior to the uterus, and was not seen at transabdominal US.

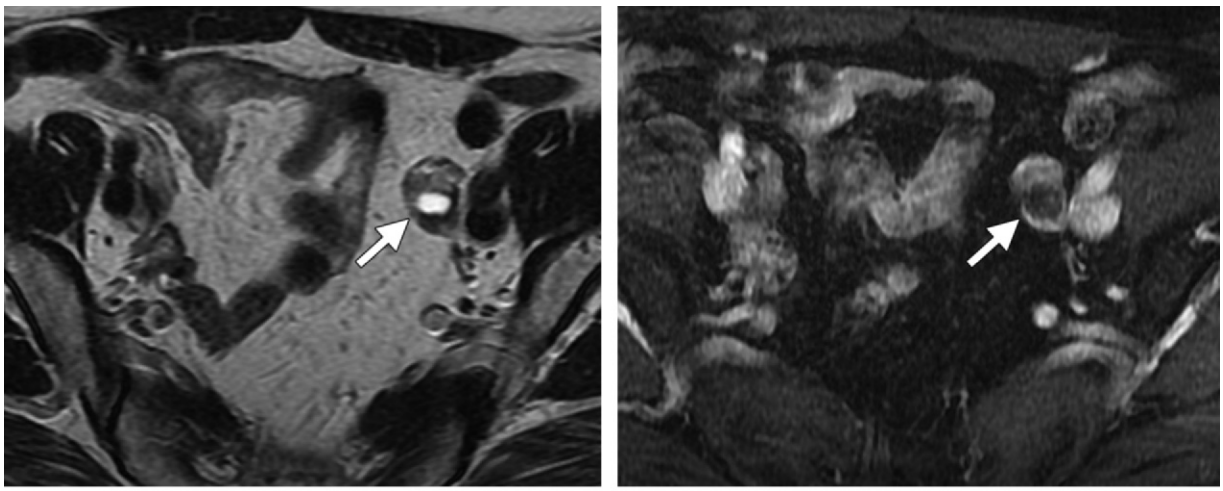

a. b.

Figure 29. Unilocular subcentimeter ovarian cyst in a 54-year-old postmenopausal woman. Axial T2-weighted **(a)** and T1-weighted fat-suppressed contrast-enhanced **(b)** MR images show a small cystic structure arising from the left ovary (arrow). No internal ovarian enhancement is identified. Note that the ovary is mildly atrophic and has intermediate instead of low T2 signal intensity in **a**, expected findings in early postmenopause.

during the reproductive years, after delivery, and in menopause is important for differentiating expected physiologic changes from pathologic conditions.

***Disclosures of Conflicts of Interest.*—B.G.C.:** *Related financial activities*: none. *Other financial activities:* expert witness for Evan Black Associates; speakers' bureau for Thomas Jefferson University. **J.E.L.:** *Related financial activities*: none. *Other financial activities:* consultant for BioClinica.

References

1. Ziereisen F, Guissard G, Damry N, Avni EF. Sonographic imaging of the paediatric female pelvis. Eur Radiol 2005;15(7):1296–1309.
2. Garel L, Dubois J, Grignon A, Filiatrault D, Van Vliet G. US of the pediatric female pelvis: a clinical perspective. RadioGraphics 2001;21(6):1393–1407.
3. Barr LL, Cohen HL. Ultrasonography of the pediatric and adolescent pelvis. In: Anderson JL, ed. Gynaecological imaging. London, England: Churchill Livingstone, 1999; 397–410.
4. Herter LD, Golendziner E, Flores JA, Becker E Jr, Spritzer PM. Ovarian and uterine sonography in healthy girls between 1 and 13 years old: correlation of findings with age and pubertal status. AJR Am J Roentgenol 2002;178(6):1531–1536.

5. Buzi F, Pilotta A, Dordoni D, Lombardi A, Zaglio S, Adlard P. Pelvic ultrasonography in normal girls and in girls with pubertal precocity. Acta Paediatr 1998;87(11):1138–1145.
6. Platt JF, Bree RL, Davidson D. Ultrasound of the normal nongravid uterus: correlation with gross and histopathology. J Clin Ultrasound 1990;18(1):15–19.
7. Merz E, Miric-Tesanic D, Bahlmann F, Weber G, Wellek S. Sonographic size of uterus and ovaries in pre- and postmenopausal women. Ultrasound Obstet Gynecol 1996;7(1):38–42.
8. Miller EI, Thomas RH, Lines P. The atrophic postmenopausal uterus. J Clin Ultrasound 1977;5(4):261–263.
9. Brandt ML, Helmrath MA. Ovarian cysts in infants and children. Semin Pediatr Surg 2005;14(2):78–85.
10. Cohen HL, Eisenberg P, Mandel F, Haller JO. Ovarian cysts are common in premenarchal girls: a sonographic study of 101 children 2–12 years old. AJR Am J Roentgenol 1992;159(1):89–91.
11. Laing FC, Townsend BA, Rodriguez JR. Ovary-containing hernia in a premature infant: sonographic diagnosis. J Ultrasound Med 2007;26(7):985–987.
12. Cohen HL, Shapiro MA, Mandel FS, Shapiro ML. Normal ovaries in neonates and infants: a sonographic study of 77 patients 1 day to 24 months old. AJR Am J Roentgenol 1993;160(3):583–586.
13. Pavlik EJ, DePriest PD, Gallion HH, et al. Ovarian volume related to age. Gynecol Oncol 2000;77(3):410–412.
14. Cohen HL, Tice HM, Mandel FS. Ovarian volumes measured by US: bigger than we think. Radiology 1990;177(1):189–192.
15. Aviram R, Gassner G, Markovitch O, Cohen I, Fishman A, Tepper R. Volumes of normal ovaries, ovaries with benign lesions, and ovaries with cancer in menopausal women: is there an optimal cut-off value to predict malignancy? J Clin Ultrasound 2008;36(1):1–5.
16. Siegel MJ. Computed tomography and magnetic resonance imaging of the pediatric and adolescent pelvis. In: Anderson JL, ed. Gynaecological imaging. London, England: Churchill Livingstone, 1999;411–431.
17. Yitta S, Hecht EM, Slywotzky CM, Bennett GL. Added value of multiplanar reformation in the multidetector CT evaluation of the female pelvis: a pictorial review. RadioGraphics 2009;29(7):1987–2003.
18. Bega G, Lev-Toaff AS, O'Kane P, Becker E Jr, Kurtz AB. Three-dimensional ultrasonography in gynecology: technical aspects and clinical applications. J Ultrasound Med 2003;22(11):1249–1269.
19. Lev-Toaff AS, Pinheiro LW, Bega G, Kurtz AB, Goldberg BB. Three-dimensional multiplanar sonohysterography: comparison with conventional two-dimensional sonohysterography and x-ray hysterosalpingography. J Ultrasound Med 2001;20(4):295–306.
20. Shi AA, Lee SI. Radiological reasoning: algorithmic workup of abnormal vaginal bleeding with endovaginal sonography and sonohysterography. AJR Am J Roentgenol 2008;191(6 suppl):S68–S73.
21. van Gestel I, Ijland MM, Hoogland HJ, Evers JLH. Endometrial wave-like activity in the non-pregnant uterus. Hum Reprod Update 2003;9(2):131–138.
22. Aboulghar M, Rizk B. Ultrasonography of the cervix. In: Rizk B, ed. Ultrasonography in reproductive medicine and infertility. New York, NY: Cambridge University Press, 2010; 103–112.
23. Randall JM, Templeton A. Transvaginal sonographic assessment of follicular and endometrial growth in spontaneous and clomiphene citrate cycles. Fertil Steril 1991;56(2):208–212.
24. Bakos O, Lundkvist O, Bergh T. Transvaginal sonographic evaluation of endometrial growth and texture in spontaneous ovulatory cycles—a descriptive study. Hum Reprod 1993;8(6):799–806.
25. Dickey RP. Ultrasonography of the endometrium. In: Rizk B, ed. Ultrasonography in reproductive medicine and infertility. New York, NY: Cambridge University Press, 2010; 97–102.
26. Fleischer AC, Kalemeris GC, Machin JE, Entman SS, James AE Jr. Sonographic depiction of normal and abnormal endometrium with histopathologic correlation. J Ultrasound Med 1986;5(8):445–452.
27. Chaudhry S, Reinhold C, Guermazi A, Khalili I, Maheshwari S. Benign and malignant diseases of the endometrium. Top Magn Reson Imaging 2003;14(4):339–357.
28. Reinhold C, McCarthy S, Bret PM, et al. Diffuse adenomyosis: comparison of endovaginal US and MR imaging with histopathologic correlation. Radiology 1996;199(1):151–158.
29. Togashi K, Nakai A, Sugimura K. Anatomy and physiology of the female pelvis: MR imaging revisited. J Magn Reson Imaging 2001;13(6):842–849.
30. Sydow BD, Seigelman ES. Uterine MRI: a review of technique and diagnosis. Appl Radiol 2008;37(10):18–29.
31. Scoutt LM, McCauley TR, Flynn SD, Luthringer DJ, McCarthy SM. Zonal anatomy of the cervix: correlation of MR imaging and histologic examination of hysterectomy specimens. Radiology 1993;186(1):159–162.
32. Yitta S, Hecht EM, Mausner EV, Bennett GL. Normal or abnormal? demystifying uterine and cervical contrast enhancement at multidetector CT. RadioGraphics 2011;31(3):647–661.
33. Ritchie WGM. Sonographic evaluation of normal and induced ovulation. Radiology 1986;161(1):1–10.
34. Brown DL. A practical approach to the ultrasound characterization of adnexal masses. Ultrasound Q 2007;23(2):87–105.
35. Levine D, Brown DL, Andreotti RF, et al. Management of asymptomatic ovarian and other adnexal cysts imaged at US: Society of Radiologists in Ultrasound consensus conference statement. Radiology 2010;256(3):943–954.
36. Zaidi J, Jurkovic D, Campbell S, Collins W, McGregor A, Tan SL. Luteinized unruptured follicle: morphology, endocrine function and blood flow changes during the menstrual cycle. Hum Reprod 1995;10(1):44–49.
37. Outwater EK, Talerman A, Dunton C. Normal adnexa uteri specimens: anatomic basis of MR imaging features. Radiology 1996;201(3):751–755.
38. Outwater EK, Mitchell DG. Normal ovaries and functional cysts: MR appearance. Radiology 1996;198(2):397–402.
39. Borders RJ, Breiman RS, Yeh BM, Qayyum A, Coakley FV. Computed tomography of corpus luteal cysts. J Comput Assist Tomogr 2004;28(3):340–342.

40. Lerman H, Metser U, Grisaru D, Fishman A, Lievshitz G, Even-Sapir E. Normal and abnormal 18F-FDG endometrial and ovarian uptake in pre- and postmenopausal patients: assessment by PET/CT. J Nucl Med 2004;45(2):266–271.
41. Mulic-Lutvica A, Bekuretsion M, Bakos O, Axelsson O. Ultrasonic evaluation of the uterus and uterine cavity after normal, vaginal delivery. Ultrasound Obstet Gynecol 2001;18(5):491–498.
42. Brown DL. Pelvic ultrasound in the postabortion and postpartum patient. Ultrasound Q 2005;21(1): 27–37.
43. Kamaya A, Ro K, Benedetti NJ, Chang PL, Desser TS. Imaging and diagnosis of postpartum complications: sonography and other imaging modalities. Ultrasound Q 2009;25(3):151–162.
44. Edwards A, Ellwood DA. Ultrasonographic evaluation of the postpartum uterus. Ultrasound Obstet Gynecol 2000;16(7):640–643.
45. Wachsberg RH, Kurtz AB, Levine CD, Solomon P, Wapner RJ. Real-time ultrasonographic analysis of the normal postpartum uterus: technique, variability, and measurements. J Ultrasound Med 1994;13 (3):215–221.
46. Wachsberg RH, Kurtz AB. Gas within the endometrial cavity at postpartum US: a normal finding after spontaneous vaginal delivery. Radiology 1992;183 (2):431–433.
47. Antonelli E, Morales MA, Dumps P, Boulvain M, Weil A. Sonographic detection of fluid collections and postoperative morbidity following cesarean section and hysterectomy. Ultrasound Obstet Gynecol 2004;23(4):388–392.
48. Garagiola DM, Tarver RD, Gibson L, Rogers RE, Wass JL. Anatomic changes in the pelvis after uncomplicated vaginal delivery: a CT study on 14 women. AJR Am J Roentgenol 1989;153(6): 1239–1241.
49. Maldjian C, Adam R, Maldjian J, Smith R. MRI appearance of the pelvis in the post cesarean-section patient. Magn Reson Imaging 1999;17(2):223–227.
50. Woo GM, Twickler DM, Stettler RW, Erdman WA, Brown CEL. The pelvis after cesarean section and vaginal delivery: normal MR findings. AJR Am J Roentgenol 1993;161(6):1249–1252.
51. Willms AB, Brown ED, Kettritz UI, Kuller JA, Semelka RC. Anatomic changes in the pelvis after uncomplicated vaginal delivery: evaluation with serial MR imaging. Radiology 1995;195(1):91–94.
52. Twickler DM, Setiawan AT, Harrell RS, Brown CEL. CT appearance of the pelvis after cesarean section. AJR Am J Roentgenol 1991;156(3):523–526.
53. Lobo RA. Menopause: endocrinology, consequences of estrogen deficiency, effects of hormone replacement therapy, treatment regimens. In: Katz VL, Lentz GM, Lobo RA, Gershenson DM, eds. Comprehensive gynecology. 5th ed. Philadelphia, Pa: Mosby, 2007; 1039–1071.
54. te Velde ER, Pearson PL. The variability of female reproductive ageing. Hum Reprod Update 2002;8 (2):141–154.
55. Kato I, Toniolo P, Akhmedkhanov A, Koenig KL, Shore R, Zeleniuch-Jacquotte A. Prospective study of factors influencing the onset of natural menopause. J Clin Epidemiol 1998;51(12):1271–1276.
56. Kaufman DW, Slone D, Rosenberg L, Miettinen OS, Shapiro S. Cigarette smoking and age at natural menopause. Am J Public Health 1980;70(4):420–422.
57. Seungdamrong A, Weiss G. Ovulation in a postmenopausal woman. Fertil Steril 2007;88(5):1438. e1–e2.
58. Occhipinti K, Kutcher R, Rosenblatt R. Sonographic appearance and significance of arcuate artery calcification. J Ultrasound Med 1991;10(2): 97–100.
59. Gerber B, Krause A, Müller H, et al. Effects of adjuvant tamoxifen on the endometrium in postmenopausal women with breast cancer: a prospective long-term study using transvaginal ultrasound. J Clin Oncol 2000;18(20):3464–3470.
60. Hann LE, Giess CS, Bach AM, Tao Y, Baum HJ, Barakat RR. Endometrial thickness in tamoxifen-treated patients: correlation with clinical and pathologic findings. AJR Am J Roentgenol 1997;168(3): 657–661.
61. Bennett GL, Andreotti RF, Lee SI, et al. ACR appropriateness criteria(®) on abnormal vaginal bleeding. J Am Coll Radiol 2011;8(7):460–468.
62. Goldstein SR. The role of transvaginal ultrasound or endometrial biopsy in the evaluation of the menopausal endometrium. Am J Obstet Gynecol 2009; 201(1):5–11.
63. Smith-Bindman R, Weiss E, Feldstein V. How thick is too thick? when endometrial thickness should prompt biopsy in postmenopausal women without vaginal bleeding. Ultrasound Obstet Gynecol 2004; 24(5):558–565.
64. Salem S. Gynecology. In: Rumack CM, Wilson SR, Charboneau JW, Levine DL, eds. Diagnostic ultrasound. 4th ed. Philadelphia, Pa: Mosby, 2011; 547–612.
65. Markovitch O, Tepper R, Fishman A, Shapira J, Aviram R, Cohen I. The value of transvaginal ultrasonography in the prediction of endometrial pathologies in asymptomatic postmenopausal breast cancer tamoxifen-treated patients. Gynecol Oncol 2004;95(3):456–462.
66. Imaoka I, Sugimura K, Masui T, Takehara Y, Ichijo K, Naito M. Abnormal uterine cavity: differential diagnosis with MR imaging. Magn Reson Imaging 1999;17(10):1445–1455.
67. Hall DA, McCarthy KA, Kopans DB. Sonographic visualization of the normal postmenopausal ovary. J Ultrasound Med 1986;5(1):9–11.
68. Kupfer MC, Ralls PW, Fu YS. Transvaginal sonographic evaluation of multiple peripherally distributed echogenic foci of the ovary: prevalence and histologic correlation. AJR Am J Roentgenol 1998;171 (2):483–486.
69. Muradali D, Colgan T, Hayeems E, Burns PN, Wilson SR. Echogenic ovarian foci without shadowing: are they caused by psammomatous calcifications? Radiology 2002;224(2):429–435.
70. Wolf SI, Gosink BB, Feldesman MR, et al. Prevalence of simple adnexal cysts in postmenopausal women. Radiology 1991;180(1):65–71.
71. Greenlee RT, Kessel B, Williams CR, et al. Prevalence, incidence, and natural history of simple ovarian cysts among women >55 years old in a large cancer screening trial. Am J Obstet Gynecol 2010; 202(4):373.e1–e9.

RadioGraphics

Imaging of the Female Pelvis through the Life Cycle

Jill E. Langer, MD • Edward R. Oliver, MD, PhD • Anna S. Lev-Toaff, MD • Beverly G. Coleman, MD

RadioGraphics 2012; 32:1575–1597 • **Published online** 10.1148/rg.326125513 • **Content Codes:** GU OB

Page 1578

Ovarian volume greater than 4 cm^3 and the presence of six or more follicles in girls younger than 7 years should raise concern for premature sexual development (5).

Page 1582

Endometrial thickness is best assessed with endovaginal US and represents the sum of the thicknesses of the two endometrial layers. The measurement is obtained on midline longitudinal images by placing cursors at the anterior and posterior endometrial-myometrial interfaces where the endometrium is widest, usually near the fundus. The central thin hyperechoic line represents the interface between the opposing anterior and posterior endometrial layers and should be continuous. Disruption of the central hyperechoic line, or heterogeneity of the endometrium, may indicate an underlying intracavitary lesion such as a polyp, myoma, or adhesion.

Page 1584

On contrast-enhanced CT scans obtained in women of reproductive age, the endometrium exhibits hypoattenuation relative to the inner myometrium during most phases of contrast enhancement, a finding that might be misinterpreted as fluid within the uterine cavity. Such misinterpretation may result in additional, unnecessary imaging examinations or intervention (Fig 12). [...] The normal cervix usually demonstrates less intense enhancement or enhances later than the uterine corpus at CT because of the relatively larger proportion of fibrous tissue in the cervix (29) (Fig 13).

Page 1586

Although the presence of a large ovarian cystic lesion raises concern for a cystic neoplasm, when no internal vascularity is noted, repeat US performed in the early proliferative phase is recommended after one or two menstrual cycles; many of these structures undergo involution, allowing the diagnosis of a follicular cyst (34).

Page 1592

A normal endovaginal sonogram in a postmenopausal patient has a high negative predictive value and high overall accuracy rate for excluding major disorders of the uterus and ovaries, with excellent pathologic correlation (61,62).